http://dx.doi.org/10.5935/0103-5053.20140247

J. Braz. Chem. Soc., Vol. 25, No. 12, 2164-2185, 2014.
Printed in Brazil - ©2014 Sociedade Brasileira de Química
0103 - 5053 $6.00+0.00

Review

Metallocene Supported on Inorganic Solid Supports: an Unfinished History

Aline C. dos Ouros,[a] Michèle O. de Souza[b] and Heloise O. Pastore[*,a]*

[a]*Micro and Mesoporous Molecular Sieves Group, Institute of Chemistry, University of Campinas, Rua Monteiro Lobato, 270, 13083-861 Campinas-SP, Brazil*

[b]*Laboratory of Reactivity and Catalysis, Institute of Chemistry, University of Rio Grande do Sul, Av. Bento Gonçalves 9500, P.O. Box 15003, 91501-970 Porto Alegre-RS, Brazil*

Muitos estudos recentes estão direcionados à área de produção de nanocompósitos poliolefínicos já que eles melhoram as propriedades dos polímeros em muitas aplicações. O desafio mais importante é a obtenção de uma boa dispersão das cargas de reforço na matriz polimérica. É consenso nos estudos realizados que a dispersão conduzida pela polimerização *in situ* é a mais eficiente, conferindo ao sistema, adicionalmente, as vantagens da catálise heterogênea. Esta contribuição oferece uma revisão bibliográfica das características das cargas de reforço mais empregadas, de sua utilização como suporte de catalisadores metalocênicos e da aplicação na produção *in situ* de nanocompósitos.

The production of polyolefin nanocomposites has been the field of many studies for improving polymer properties for many applications. The most important challenge on the area is the preparation of the fillers randomly dispersed on polymer matrix. It is general agreement, however, that the dispersion obtained through *in situ* polymerization is the most efficient and, additionally, confers to the system the advantages of heterogeneous catalysis. This contribution offer a review of characteristics of the most employed fillers, their use as metallocene catalysts supports and the application on *in situ* production of nanocomposites.

Keywords: polymer nanocomposites, metallocene catalyst, *in situ* polymerization, polyolefin, inorganic nanoparticles

1. Introduction

Polyolefins compose more than 60% of polymer production in the world nowadays.[1] The most important characteristic for this success are the highest turnover of all polymers, low cost, abundance of the monomers and easy processability and long durability.[1-3] These characteristics make polyolefins valuable for applications in many industrial fields. Despite all these properties, they present certain limitations in some applications, including those which require improved mechanical properties, decreased gas permeability and flammability, and increased biodegradability.

For years, addition of fillers and reinforcements to produce polyolefin nanocomposites (NCs) have been used as an alternative to extend the use of these polymers,[4-9] improving their mechanical and physicochemical properties for many applications, which favors, for example, the use of these polymeric nanocomposites as replacement for materials like metals, glass and ceramics, and thus decreasing the costs. Polyolefin nanocomposites seem to be the next innovation to potentially bring novel properties and characteristics.[10]

One of the most important features that determines the nanocomposite properties is the kind of filler used in their formulation. Many considerations must be taken into account before choosing a filler that, into the polymer matrix, is supposed to produce a certain property as a composite. Some important characteristics of the filler to take into consideration are the chemical surface composition, size and shape of the nanoparticles, structure, pore sizes, interlayer distances, hydrophobicity and mechanical, electrical and thermal properties. The most used particles are silicates (phyllosilicates or lamellar silicates), polyhedral oligomeric silsesquioxane (POSS), carbon nanotubes, metal and/or other inorganic

*e-mail: gpmmm@iqm.unicamp.br

nanoparticles and polymeric fibers.[11] New studies involve the production of different and specific fillers, for example, an interesting material for electronic industries was developed by Morelos-Gómez *et al.*,[12] the graphene nanoribbons (GNRs), made of carbon nanotubes ribbons opened in a non-oxidative way.

Since the successful synthesis of nylon-clay nanocomposites by Toyota researchers,[13,14] the use of layered materials as fillers in polyolefin NCs presents a great deal of interest and it is the most studied family of fillers for NCs. This success is probably due to the great improvement on NC's mechanical, thermal and barrier resistance against permeation of gases shown in many publications.[15-17]

Other important characteristic that set new properties for NCs is the filler dispersion defined mainly by the type of NC preparation. The production by melt compounding of nonpolar chains, such as polyolefins, leads to an insufficient filler dispersion and then aggregation of the layers, which can deteriorate the mechanical properties of the polymer. This disadvantage can be solved by an *in situ* polymerization leading to the exfoliation of the filler in the polymer matrix during the polymerization process.[18,19] *In situ* intercalative polymerization starts with the intercalation of the monomer into the interlayer space of the layered material and the beginning of the polymerization process followed by the growth of the polymer chains promoting exfoliation of the lamellas.

Additionally, the industrial production of polyolefins uses mostly heterogeneous catalysis, where the catalysts are found fixed in a support. After the advent of Ziegler Natta catalysts,[20,21] and still nowadays, many studies involving catalysts for polyolefin production are developed. Throughout this time, different complexes were investigated,[22] among them, the metallocene catalysts. Metallocene complexes made important contributions for the polyolefin field,[23] by producing polymers with new properties and therefore, new applications for them. Their molecular characteristics as aromatic ligands, bridged or not, and the nature of the metal are parameters to control the polymerization, creating polymers with specific stereospecificity (when PP is produced) and polydispersity and providing the preparation of block copolymers.[24-27]

Considering these important topics, this contribution has the objective of reviewing the literature from the pioneer publications to nowadays, on nanocomposite production, especially using *in situ* polymerization catalysis by metallocene supported on different inorganic solid supports for the nanocomposite production. Other preparation methods are also discussed for comparison. The next section, numbered 2, deals with a review of metallocene catalysts and the one on inorganic support materials for these catalysts can be read in section 3. The preparation of nanocomposites by several methods is found in section 4. The morphology and NC's properties are discussed in section 5.

2. Metallocene Catalysts

The remarkable advances on polyolefin catalysis made by Ziegler and Natta during the 1950s, stimulated researches on novel catalysts for polyolefin production.[28,29] The first-generation catalysts were based on $3TiCl_3$, $AlCl_3$ and $Al(C_2H_5)_2Cl$ and allowed the preparation of polypropene (PP), however with low activity.[30] Other generations of catalysts came, Table 1 summarizes the results.[29]

The first use of metallocene catalyst in the production of polyethylene (PE) was reported in the 1950s by Breslow and Natta.[20,21] The catalyst was Cp_2TiCl_2 (Cp = cyclopentadienyl) activated by mixed aluminium alkyl halides in a homogeneous system. This system presented low activity and demanded improvement. Sinn and Kaminsky[31] demonstrated better activities by using methylalumoxane (MAO) as cocatalyst for this system. Isotactic PP was obtained for the first time by Brintzinger and co-workers,[32] using ansa-bis(indenyl) complexes in a racemic (rac) mixture. After that (in 1988), Razavi and co-workers,[33] synthesized an ansa-metallocene complex $[ZrC_5H_4CMe_2C_{13}H_8C_{12}]$ that favored the production of syndiotactic PP with high activity (order of 10^3 kg PP mol^{-1} h^{-1}).

As made clear above, activation of metallocene is necessary to obtain good activities; MAO proved to be the best cocatalyst by forming a cationic metallocene active species in olefin polymerization. The chemical nature of MAO is still not quite clear. Aluminum and oxygen atoms form a chain and free valences in aluminum are saturated by methyl substituents to form linear-[MeAlO]n-units, where n varies from 5 to 20.[34,35] Besides this linear form, cyclic and associated species (Figure 1), were also found; these can aggregate to cages.

The interest in supporting the metallocene catalyst comes from the fact that the homogeneous system would find difficulties to be used in industrial plants that operate with heterogeneous Ziegler-Natta and Phillips catalyst.[36] Homogeneous metallocene catalysts present high activities and stereospecificities for the polymerization of prochiral olefins. As the polyolefin deposits at reactor walls causing boiler scale effect, i.e., changing drastically the mass and heat transfer, a continuous process would not be possible.[37] It was also found that the polymers produced by the

Table 1. Performance of different catalyst generations. Reprinted from reference 29. Copyright 2014, with permission from Elsevier

Generation	Composition and structure	Productivity / (kg PP g^{-1} Cat)	II / wt.%[a]	Technology control	Process requirements
1st (1957-1970)	$3TiCl_3Al_3/AlEt_2Cl$	0.8-1.2	88-91	Irregular powder	Need of purification and atactic removal
2nd (1970-1978)	$TiCl_3/AlEt_2Cl$	3-5	95	Irregular powder	Need of purification and atactic removal
3rd (1978-1980)	$TiCl_4$/ester/$MgCl_2$ + $AlEt_3$/ester	5-15	98	Regular/irregular powder	No purification, need of atactic removal
4th (1980) RGT[b]	$TiCl_4$/diester/$MgCl_2$ + $AlEt_3$/silane three-dimensional catalyst granule architecture	20-60	99	Particles with regular shape and adjustable size and PSD[e]. Designed distribution of the different products inside each particle	No purification. No atactic removal. No pelletisation
	$TiCl_4$/diether/$MgCl_2$ + $AlEt_3$ three-dimensional catalyst granule archieture	50-120	99	Particles with regular shape and adjustable size and PSD. Designed distribution of the different products inside each particle	No purification. No atatic removal. No pelletisation
5th metallocenes 6th multicatalyst RGT	zirconocene + MAO[c] mixed catalysis: ZN[d] + radical initiators, ZN + single site (catalysts)	(5-9) × 10^3 (on Zr)	90-99	To be improved Particles with designed distribution of both olefinic and non-olefinic materials	–

[a]II = isotacticity index; [b]RGT = reactor granule technology; [c]MAO = methylaluminoxane; [d]ZN = Ziegler-Natta; [e]PSD = particle size distribution.

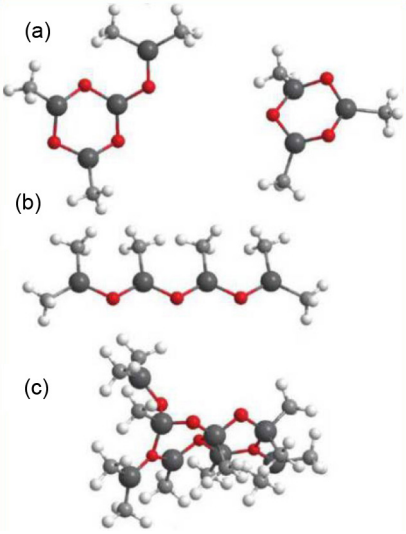

Figure 1. Unit cyclic (a), linear (b), and associate (c) structures of MAO; red balls: oxygen; gray balls: aluminum and methyl groups. Reprinted with permission from reference 35. Copyright 2014 American Chemical Society.

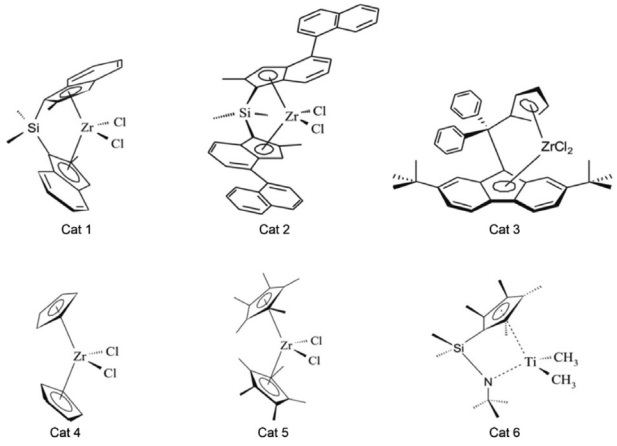

Figure 2. Structures of metallocenes used for the synthesis of PP and PE.[3]

homogeneous metallocene system have narrow molecular weight (Mw) distributions, which sets good mechanical properties, but hampers polymer processing.[38]

Figure 2 shows some metallocenes used in heterogeneous catalysis, where MAO is cocatalyst, to produce PE or PP. Cat1 and Cat2 produce isotactic PP, while Cat3 produces syndiotactic PP and Cat4 atactic PP. All of these metallocenes are also able to synthesize PE.[3]

3. Inorganic Support Materials

The most representative examples of inorganic support materials used for Ziegler-Natta and Phillips catalysts are silica, alumina and magnesium dichloride.[36] The importance of the support on activity and polymer properties is remarkable. The support can change profoundly the nature of active sites on the catalyst, which also reflects in polymer properties as molecular weight, polydispersity index and stereospecificity (when PP is produced).[36] The catalyst thermal stability can also be improved by heterogenization. Freitas *et al.*[39] showed that, when $Ph_2C(Cp)(Flu)ZrCl_2$ (flu = fluorenyl) is immobilized on silica, the thermal

stability is improved. The activity that decreases with increase in the temperature reaction on homogeneous system, suffers less influence when the polymerization is performed under heterogeneous conditions. Another characteristic of the inorganic supports is the possibility to control the morphology of particles aiming at the protection of the reactor from fouling.[40]

Several studies are devoted to finding a support for metallocene that could improve or, at least, maintain the homogeneous characteristics. To reach such challenge, the attention is directed to the development of both immobilization methods and supports. Figure 3 shows important members of nanoparticle families used for *in situ* composite formation.[41] In the rest of section 3, the discussion will be directed to the main properties of the most used supports.

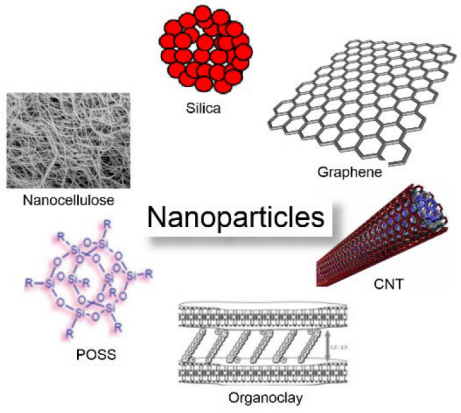

Figure 3. Nanofiller families including molecules and inorganic nanoparticles. Adapted from reference 41.

3.1. Porous materials

The most frequently used porous supports are inorganic oxides like silica, alumina or aluminosilicates. These materials are largely used because of low-cost, varied morphologies and particle sizes, and high surface areas (ca. 10^2 m^2 g^{-1}). Their surface chemistry, that basically contains OH groups whose acidity can be designed and identified, are versatile enough to allow the heterogenization of the catalytic system using several methods.[1,42-44]

The review of the literature shows many studies using micrometer particles of silica as metallocene supports,[45-48] when compared with the respective homogeneous system, they show lower activity. Nanometric silica particles on the other hand, besides producing nanocomposites, showed higher ethylene polymerization activities than microsized catalysts under identical reactions conditions.[49-52] A study that tested both metallocene supported in microsized and nanosized silica particles evaluated the influence of particle size on supported metallocene activity in production of PP.[53] For that, the authors supported rac-ethylenebis(1-indenyl) zirconium (IV) dichloride (rac-Et[Ind]$_2$ZrCl$_2$) on both MAO pretreated silica supports (by reaction in toluene at 70 °C for 16 h). The samples were tested with and without the addition of external MAO solution in the reaction mixture ([Al]/[Zr] = 570 and 17, respectively). Figure 4a shows the activity results using metallocene supported on both silica supports at the ratio [Al]/[Zr] = 570 and Figure 4b at [Al]/[Zr] = 17. These results clearly show that the nanosized catalyst had significantly better polymerization activity than the microsized catalyst in the studied range of temperature. No significante influence caused by the catalyst support size was found on the effects of polymerization temperature on polymerization activity.

Another way to increase the activity of silica supported metallocene catalysts is to add Lewis or Brönsted acid functionalities. Acidic sites allow activating the metallocene by stabilizing the ionic pair formed by the cationic zirconocene and the chlorinated MAO species. One way to make it possible is to graft sulfonic groups on mesoporous

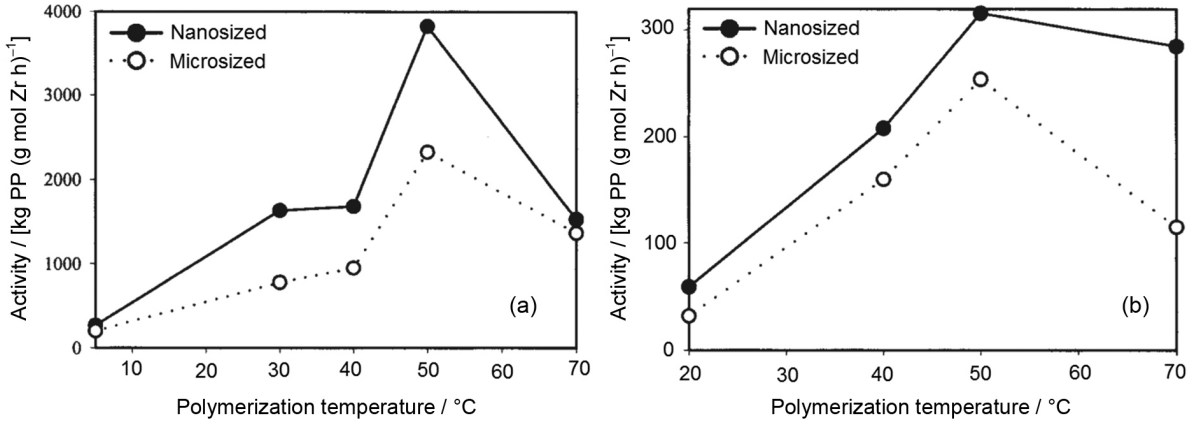

Figure 4. Polymer activity as a function of polymerization temperature for the nanosized and the microsized catalysts with 2 h of polymerization time; (a) [Al]/[Zr] = 570 and (b) [Al]/[Zr] = 17. Adapted from reference 53.

silica. When the solid presents strong Brönsted acid sites, it may be able to polymerize ethylene in the absence of the common cocatalyst MAO.[54-56] A schematic demonstration of the interactions of metallocene Cp_2ZrCl_2 with species present in neutral or acidic silicate surfaces is shown in Figure 5.

Casas *et al.*[24] supported MAO-(nBuCp)$_2$ZrCl$_2$ in mesoporous silica-alumina functionalized with propyl sulfonic acid groups in two different concentrations, 10 wt.% [meso-SiO_2-Al_2O_3/Pr(10)] and 20 wt.% [meso-SiO_2-Al_2O_3/Pr(20)]. They also produced supported MAO-(nBuCp$_2$)ZrCl$_2$ in Al-SBA-15 pure and functionalized with propyl sulfonic acid groups using 20 wt.% [SBA-15/Pr(20)]. They used these samples as heterogeneous catalysts for ethylene polymerization. The results are shown in Table 2.

When mesoporous silica-alumina (Si/Al = 25) was functionalized with 10 wt.% of propylsulfonic groups, a remarkable activity is obtained. The authors first considered that the higher activity of this catalyst, comparing with the more functionalized one (20 wt.%), might be related to the presence of higher pore volume. However, they noticed that in previous results, using 10 wt.% propyl sulfonic SBA-15 as a support, lower activity than 20 wt.% propyl sulfonic SBA-15 was obtained, indicating that the porosity was not the main factor affecting the activity. The type of acidity might play the key role. According to the authors, when meso-SiO_2.Al_2O_3/Pr(20), which contained only extra framework aluminium (Lewis acid sites) is used, a lower catalytic activity by comparison with the SBA-15/Pr(20) sample is observed. Thereby, the sample meso-SiO_2.Al_2O_3/Pr(10) contains inside framework aluminium. This aluminium is supposed to have partly the Brönsted acid character, which adds up to the Brönsted acid sites of the propyl sulfonic acid groups, causing a cooperative effect.

The first use of zeolites as supports for metallocene catalysts was reported in 1994, when Ciardelli and

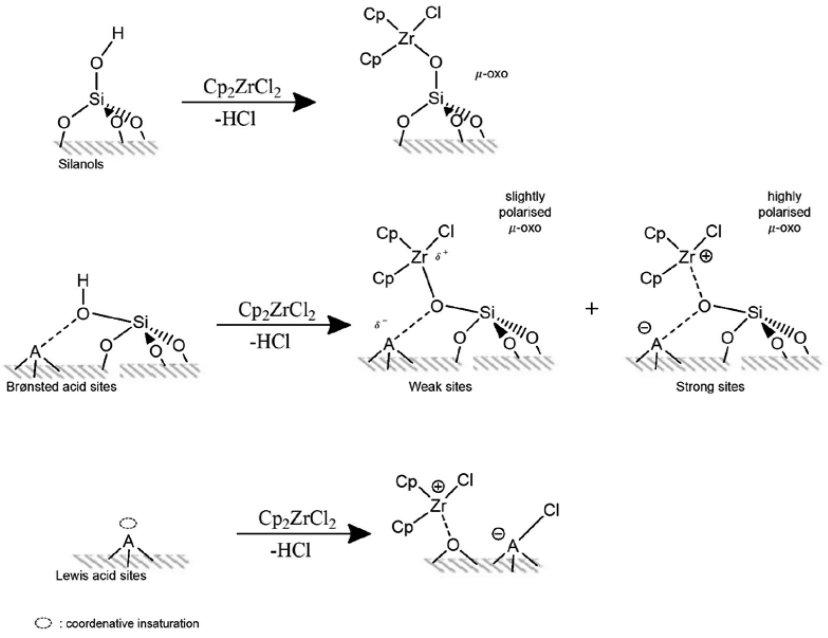

Figure 5. Models for the interactions of metallocene Cp_2ZrCl_2 with species present in acidic silicate surfaces (A: acidic element). Reprinted from reference 57. Copyright 2014, with permission from Elsevier.

Table 2. Reaction results obtained by the ethylene polymerization over the studied catalysts. Reproduced from reference 24 with permission from The Royal Society of Chemistry

Catalyst	Zr[a] / wt.%	Al/Zr molar ratio[a]	Activity[b]	Leaching[b]	M_w^c/ (g mol^{-1})
Al-SBA-15	0.56	126	1045	271	222 400
SBA-15/Pr(20)	0.33	196	3430	282	329 000
Meso-SiO_2.Al_2O_3/Pr(10)	0.57	98	4593	293	167 000
Meso-SiO_2.Al_2O_3/Pr(20)	0.43	153	2405	240	272 100
Homogeneous[d]	–	–	4440	–	65 00

[a]Determined by ICP analysis; [b]kg PE mol$_{Zr}^{-1}$ h^{-1} bar^{-1}. Polymerizarion conditions: m_{cat} = 30 mg; $V_{n\text{-heptane}}$ = 600 mL; P = 8 bar; T = 85 °C; time = 30 min; N = 900 rpm; MAO solution/Zr = 800; [c]determined by GPC; [d]measured at 70 °C.

Arribas[58] impregnated Cp_2ZrCl_2 directly on the HY zeolite. The resulting supported catalyst was active in ethylene polymerization in the presence of MAO, but with lower values than the homogeneous equivalent catalyst. The authors attributed the lower activity to the interaction of metallocene with the silanols present in the zeolite. They proved the hypothesis by reacting the support with trimethylaluminium (TMA) that converts the silanols into Si-$AlMe_2$ groups. After that, zirconocene dichloride was impregnated on the silanol-suppressed zeolite and the activity increased to a value close to that obtained for the homogeneous catalyst.

Metallocene supported in mesoporous silicas was studied for the first time by Maschmeyer *et al.*.[59] By the diffusion of a chloroform titanocene dichloride solution into the pores of MCM-41, they grafted titanocene complex on the walls of MCM-41, resulting in a well dispersed material with high surface concentration of Ti. In another study,[60] this group showed that the ligand structure (electron-donating groups bonded to the metal) is preserved after the direct impregnation of MCM-41 with Cp_2TiCl_2 solutions. In other words, the carbon framework has remained in the metallocene. It was shown that using this support, the ligand structure of impregnated metallocene remains unchanged and that the active cationic surface species after impregnation with different metallocenes are preserved.[61,62] The schematic demonstration of the interaction of metallocene with MCM-41 and followed addition of MAO are shown in Figure 6.

A study that used silica and alumina supports for a Cp_2ZrCl_2 and $(n\text{BuCp})_2ZrCl_2$ mixtures showed how the internal environment inside the pores of the supports and its polarity affect the molecular structure of the grafted metallocenes.[63,64] It was proposed that smaller pores that contain higher density of silanol groups have stronger interaction with the coordination sphere around the Zr centre, increasing the Zr-C distances. Such an increase would influence the olefin coordination and chain propagation steps, which in turn, would affect the overall catalyst activity. This proposition is depicted in Figure 7a. The authors defended that the increase in the Zr-C distances, decreases the catalyst activity. Figure 7b shows the relationship between Zr-C interatomic distance and catalyst activity. Another study,[60] that aimed the structural characterisation of rac-ethylenebis(1-indenyl) zirconium dichloride bounded to the surface of MAO

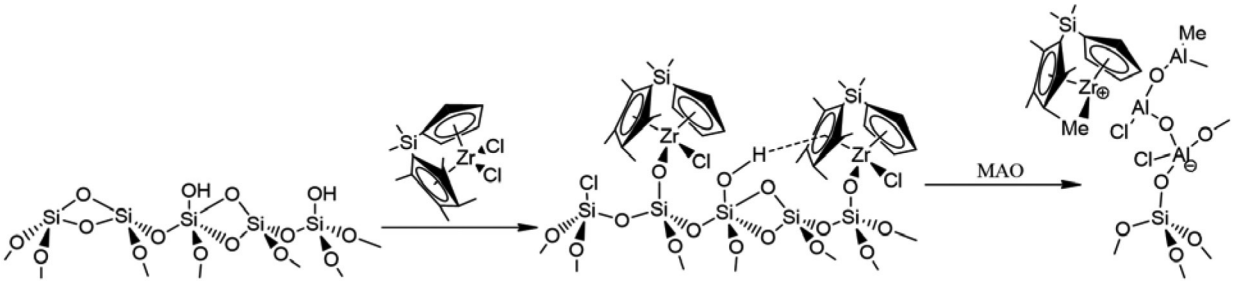

Figure 6. Interaction of MCM-41 with a metallocene, followed by MAO. Reprinted from reference 61. Copyright 2014, with permission from Elsevier.

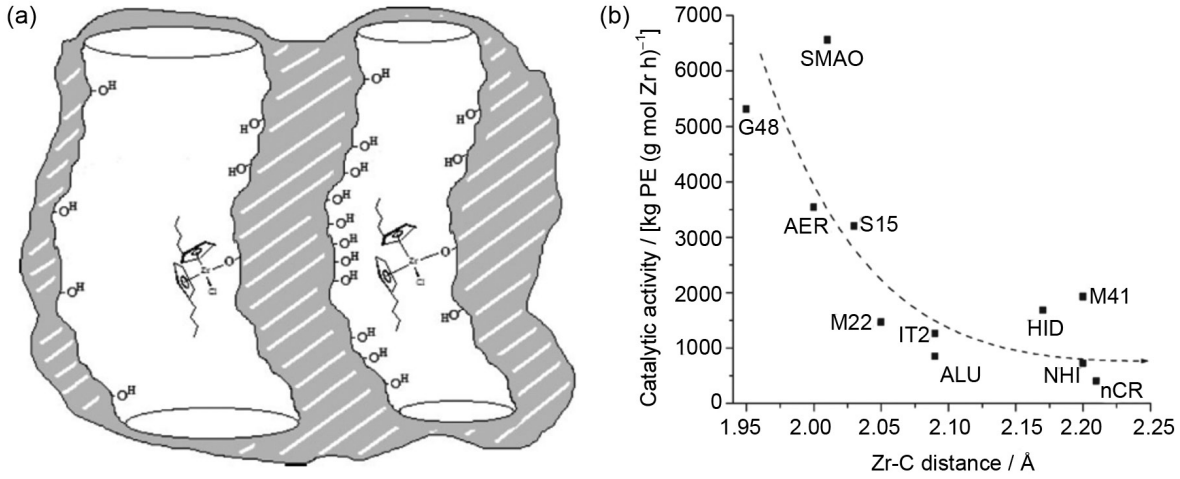

Figure 7. (a) Proposed interaction between grafted metallocene species within larger and smaller diameter pores. (b) Correlation between Zr-C interatomic distance and catalyst activity. Adapted from reference 63.

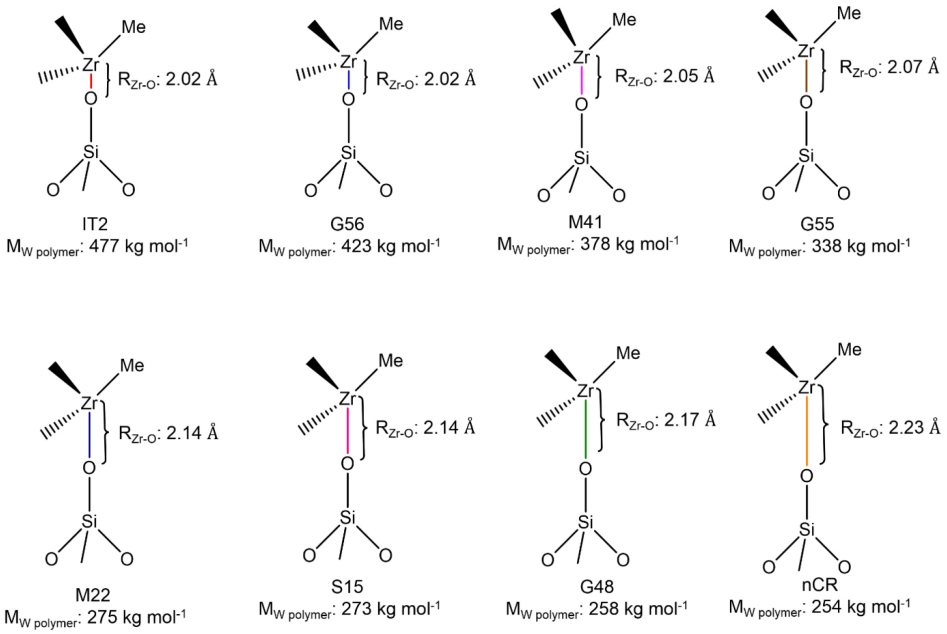

Figure 8. Correlation between the mean Zr-O interatomic distance in the grafted species and the Mw of the resulting PE. Reprinted with permission from reference 63. Copyright (c) 2014 [John Wiley and Sons, Inc.].

modified MCM-41, proposed that a short Zr-C bond is an indicative of the increased charge at the metal centre as a result of the interaction between the metal chloride and the support.

Considerations about the distances between Zr centre and support surfaces indicated that the catalysts with shorter Zr-O bonds produce PEs with higher molecular weight. Silveira *et al.*[63] suggested that, when the metallocene species are less hindered by the surface (i.e., increasing Zr-O distance), chain termination step is favored, thereby causing a decrease in the Mw of the produced polymer.[63] Figure 8 shows the correlation between mean Zr-O interatomic distance and the Mw of the resulting PE.

It is noted that the presence of structural aluminum on the support have a strong influence over the polymerization catalyst since it leads to different sorts of surface acidity in the material. Many studies investigated the influence of the Si/Al molar ratios in olefin polymerization.[57,65-71] Moreover, for some of these materials, the acidity characterization can be found in the literature,[72,73] which helps in choosing the support depending on the desired activity or/and final polymer properties. From these studies,[24,54-57,65-71] it can be concluded that the presence of an acidic element in the framework of the support of metallocene polymerization catalysts acts in order to improve the activity of the systems.

Polymers prepared with mesoporous supports can exhibit a fibrous morphology after their formation inside of the pores. The first report of this occurrence was made by Kageyama *et al.*,[74,75] that named this phenomena as extrusive polymerisation. Cp_2TiCl_2 was immobilized on mesoporous silica fibres (pore diameters 27 Å, arranged in a parallel direction to the fiber axis) in combination with MAO. After the production of high Mw PEs, they found by scanning electron microscopy (SEM) micrographs of the freeze-dried PE, bundles of PE fibers (Figure 9A and 9B). The magnification of the view (field emission SEM), shows ultrathin discrete fibers with 30 to 50 nm in diameter (Figure 9C).[74] The extrusion polymerization mechanism, postulated by the authors, is shown in Figure 10. The mesopores served as a template, suppressing the kinetically favored chain folding process.

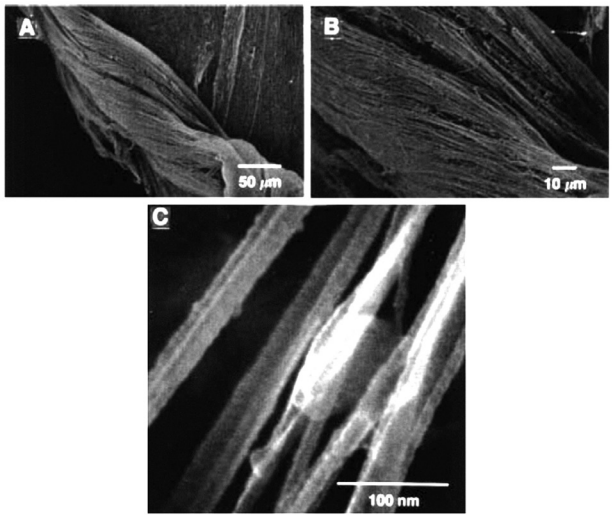

Figure 9. (A to C) SEM images of freeze-dried PE at three different magnifications. From reference 74. Reprinted with permission from AAAS.

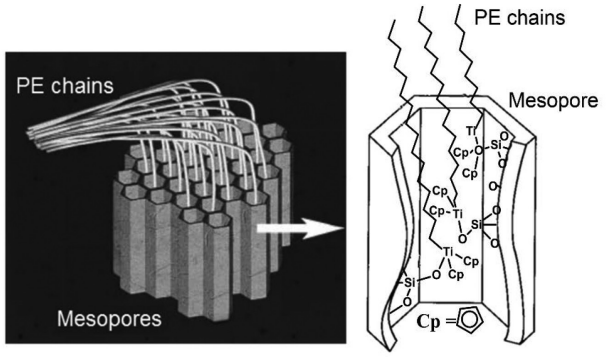

Figure 10. Conceptual scheme for the growth of crystalline fibers of PE by mesoporous silica-assisted extrusion polymerization. From reference 74. Reprinted with permission from AAAS.

3.2. Carbon nanotubes

After their discovery by Ijima,[76] carbon nanotubes (CNTs) have attracted intense attention from academics and industrials, all because of their unique mechanical thermal and electrical properties.[77,78] These outstanding properties made CNTs attractive materials in a wide range of areas. Polymer nanocomposites using CNTs as fillers represent a new class of materials with remarkable thermo-mechanical performances. *In situ* ethylene polymerization was made[79] using Cp_2ZrCl_2 adsorbed onto multiwalled carbon nanotubes (MWCNT). Cp_2ZrCl_2-MWCNT (Figure 11) was obtained by simple mixing in tetrahydrofuran (THF) at room temperature. The adsorbed Cp_2ZrCl_2 was not removed by washing with THF and toluene. This catalyst produced a high molar weight PE ($\overline{M}_w$ = 1,000,000 g mol^{-1}). The authors consider that the polydispersity index (PDI) of 2 indicates only one Zr-based chemical species of adsorbed catalyst.

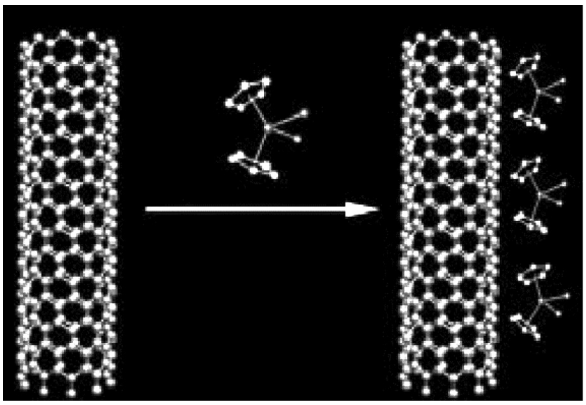

Figure 11. Preparation of Cp_2ZrCl_2-MWCNT. Reprinted with permission from reference 79. Copyright (c) 2014 [John Wiley and Sons, Inc.].

Dubois *et al.*[80] treated nanotube surface with a highly active metallocene-based complex, rac-Et(Ind)$_2$ZrCl$_2$/modified MAO (MMAO-3A) for *in situ* copolymerization of ethylene (E) and 2-norbornene (N). The de-aggregation of the carbon tubes was successfull and after further melt blending with ethylene-vinyl acetate copolymer (27 wt.% vinyl acetate) matrix, a high-performance polyolefinic nanocomposite was produced with mechanical properties being significantly enhanced. In another study, Dubois *et al.*[81] aiming at breaking up of the native nanotube bundles, used the *in situ* copolymerization of ethylene (E) and 2-norbornene (N) method that produced homogeneous surface coating of MWCNTs by the polymer. The nanotube surface was first activated by MAO and then submitted to the fixation of the bis(pentamethyl-η^5-cyclopentadienyl)zirconium(IV) dichloride ($Cp^*_2ZrCl_2$) catalyst onto the surface-activated carbon nanotubes. After all, the *in situ* polymerization promotes the de-aggregation of carbon nanotubes and its coating by the polymer matrix. The schematic procedures for this method are shown in Figure 12A. The morphology of the coated MWNTs evaluated by transmission electron microscopy (TEM) (Figure 12B) showed that MWCNTs were relatively well separated in comparison with the starting highly entangled bundle-like associations, and covered by homogeneous E-N copolymer layer.

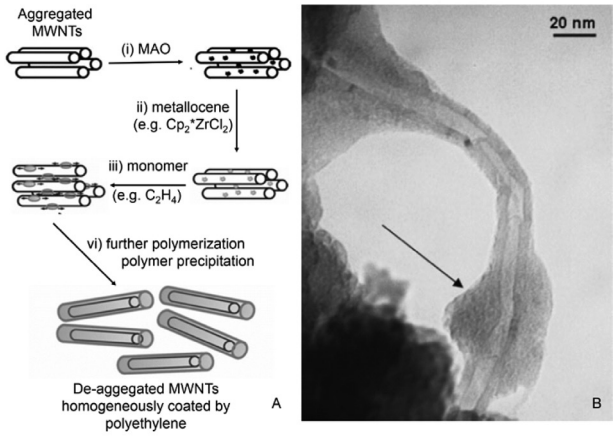

Figure 12. (A) Scheme of homogeneous surface coating of MWCNTs caused by *in situ* polymerization. (B) TEM micrographs of MWNTs coated by *in situ* grown E-N copolymers (highlighted by the arrow) (45 wt.% E-N). Adapted from references 80 and 81.

For nanocomposites production, surface modifications on CNTs can be made in order to make them more compatible with the polymer matrix. Two different approaches for the surface modification of CNTs are adopted: covalent and noncovalent; depending on whether or not covalent bonding between the CNTs and the functional groups and/or modifier molecules is involved in the modification surface process.[82] Figure 13 shows a typical representation of such surface modifications.

Park and Choi[83] proposed a simple but versatile method to produce nanocomposites of a high Mw PE filled with MWCNT by the adsorption of half-titanocenes onto

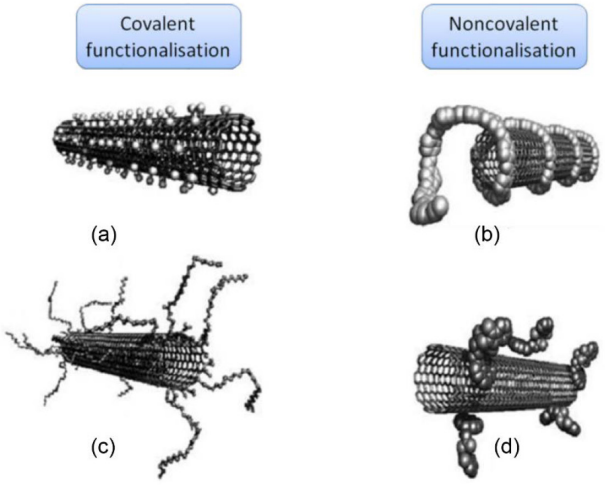

Figure 13. Different routes for nanotubes' functionalization: sidewall covalent functionalization (a); defect-group covalent functionalization (b); noncovalent polymer wrapping (c); noncovalent pi-stacking (d).[82]

MWCNTs. As a differentiation of others CNT-supported catalytic systems, they used CNTs as an "external" ligand as well as a support, while other systems use CNTs only as a support. The authors believe that using a method involving neither the chemical treatment of CNTs, nor covalent bonding would be beneficial in industrial processing and other applications.

3.3. Layered materials

Polymer-layered silicate (PLS) nanocomposites gained momentum for two major findings that stimulated the interest in these materials. First because Toyota's group[13,14] developed a promissor material composed by Nylon-6 (N6)/clay nanocomposite in which individual silicate layers of about 1 nm thickness are completely dispersed in N6 matrix. In this study, very small amount of loaded layered silicate were enough to promote pronounced improvement on thermal and mechanical properties. Then, Vaia *et al.*[84] observed that it is possible to melt-mix polymers with layered silicates, without the use of organic solvents.

The main advantages of PLS nanocomposites are: ultrafine phase dimensions promoted by the two-dimension filler, high aspect ratio of the layers that provides a large surface area contact and the improved properties of the nanocomposites using this material.[5,85] Depending on the interfacial interactions between the polymer matrix and the layered silicate, for example the 2:1 phyllosilicates whose structure is shown in Figure 14, three different types of PLS nanocomposites can thermodynamically be prepared. However, to produce a truly nanocomposite, with reproducible and homogeneous

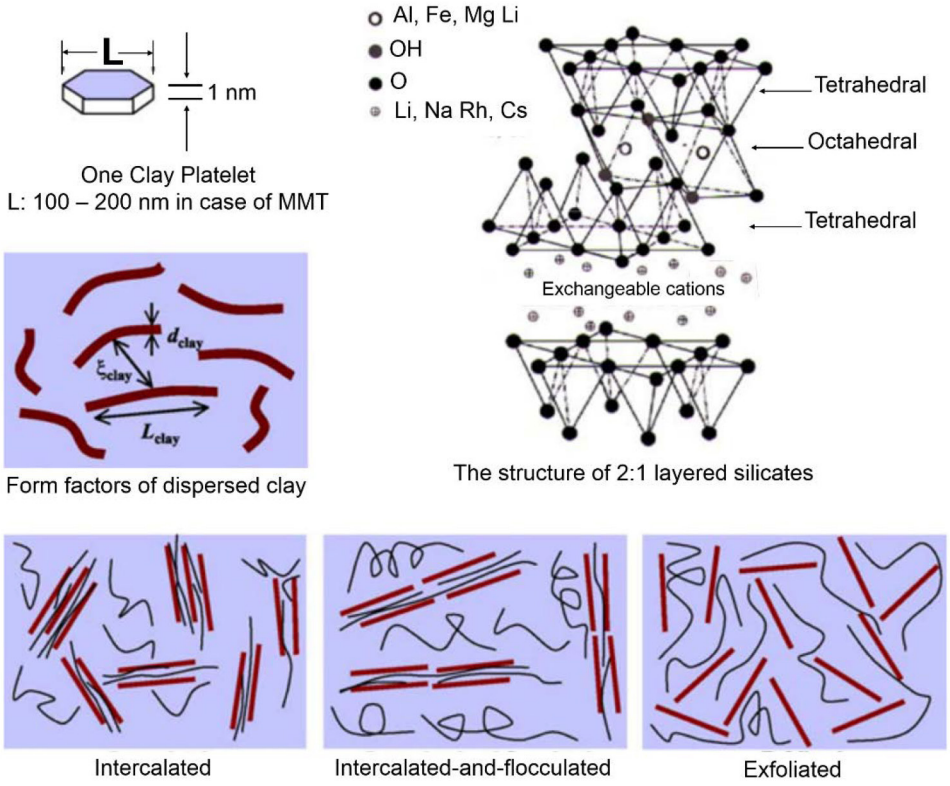

Figure 14. Structure of 2:1 phyllosilicates and schematically illustration of clay form factors of dispersed clay and the three different types of thermodynamically achievable polymer/layered silicate nanocomposites. Reprinted with permission from reference 86. Copyright 2014 American Chemical Society.

properties, exfoliation of the layers into the polymer matrix is required, this is possible by a good interaction of layer-polymer chain.

Despite the numerous clays advantages [large interlayer surface area (ca. 700 $m^2 g^{-1}$), high cation exchange capacity (ca. 100 mol kg^{-1}), expansion in water, and tendency for intercalating organic molecules], montmorillonites (MMTs) and related phyllosilicates present hydrophilic surfaces because of the presence of hydrated inorganic counterions such as Na^+ and Ca^{2+} in the interlayer space.[87] These surfaces are immiscible with the hydrophobic polymers. To minimize the incompatibility, studies propose many clay treatments that are supposed to increase the polymer-clay nanocomposite interaction. The three more used clay surface modifications are: organic modification of the clay, thermal treatment of the clay, and treatment of clay with alkylaluminum compounds. These processes will be explained in more detail belows.

3.3.1. Clay organic modification

Replacement of inorganic exchange cations on the clay surface by cationic surfactants helps making the clay compatible with the polymer matrix. The most used surfactants for this objective are quaternary alkylammonium, quaternary alkylphosphonium, imidazolium, and pyridinium salts.[5,88] This treatment reduces the polarity of the clay surface and increases the interlayer space, which enables catalyst incorporation in the anchoring points.[89] An application example is shown in Figure 15, where, as a first step, the organoclay, i.e., alkylammonium-exchanged MMT, is swelled in alcohol, e.g., *n*-butanol, and incorporates the alkoxide, e.g., tetramethoxysilane (TMOS) or tetraethoxysilane (TEOS). In a second step, water is added to produce the hydrolysis/condensation of the alkoxide. Convenient thermal treatment drives to the subsequent elimination of the alkylammonium chains by pyrolysis/combustion, leading to delamination of the clay-nanoparticles materials.

3.3.2. Thermal treatment

The clay thermal treatment is necessary since the water present on the clays acts as a poison to the metallocene catalyst, leading to deactivation and then, the non-exfoliation of the layers upon polymerization. The organo modification of the clay can decrease the water content considerably,[91] however, it is still large enough in the form of structural water to cause significant catalyst deactivation.

3.3.3. Treatment with alkylaluminum compounds

If the temperature to eliminate water is so high as to cause the collapse of support's structure, the hidrophobization with alkylaluminum compounds such as MAO, TMA, triethylaluminium (TEA) and triisobutylaluminium (TIBA) can allow a moderate thermal treatment to remove the residual water on the clay,[92] preserving its structure. A scheme with the representation of surface modification of clay with quaternary and tertiary ammonium salts are shown in Figure 16.

3.4. Metallocene supporting

The first reported method in which the filler surfaces were treated with metallocene-based catalyst for the production of polyolefins in the presence of the filler was made by Kaminsky.[94] By this method, the clay surface is treated with an alkylaluminum compound to reduce the water content, and then, the catalyst or cocatalyst solution is impregnated onto the clay surface. A proposed scheme of the reactions during catalyst supporting on Cloisite 93A is shown in Figure 17. This is the most used technique for the *in situ* synthesis of polymer/clay nanocomposites using metallocene catalysts.[93,95-97]

Ren *et al.*[98] reported a method in which MMTs were intercalated with a polimerizable agent, undec-10-enylammonium chloride, to produce polymerizable montmorillonites (P-MMTs). P-MMTs were chemically

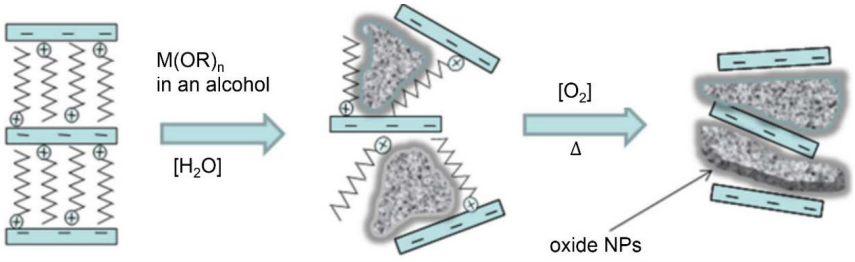

Figure 15. Scheme of the delamination of alkylammonium-exchanged layered clays (on the left) with alkoxides following a sol-gel process giving rise to intermediate organo-clay materials that after thermal treatment (> 450 °C) in the presence of oxygen leads in a second step to delaminated clay-nanoparticles (NPs) materials. Reproduced from reference 90 with permission from The Royal Society of Chemistry.

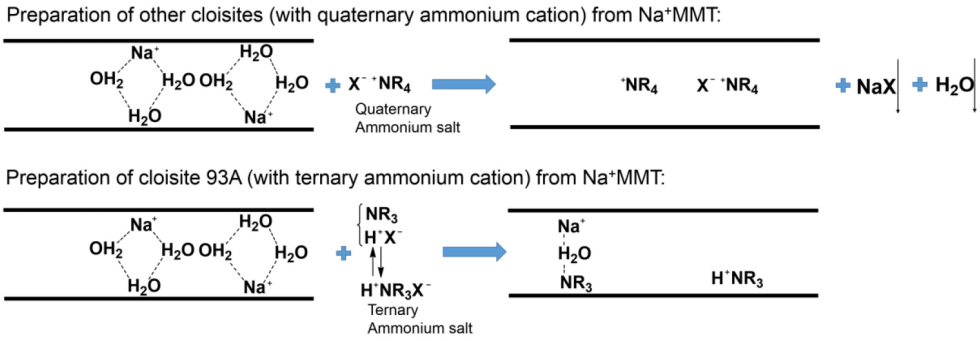

Figure 16. Surface modification of clay with quaternary and tertiary ammonium salts. Adapted from reference 93.

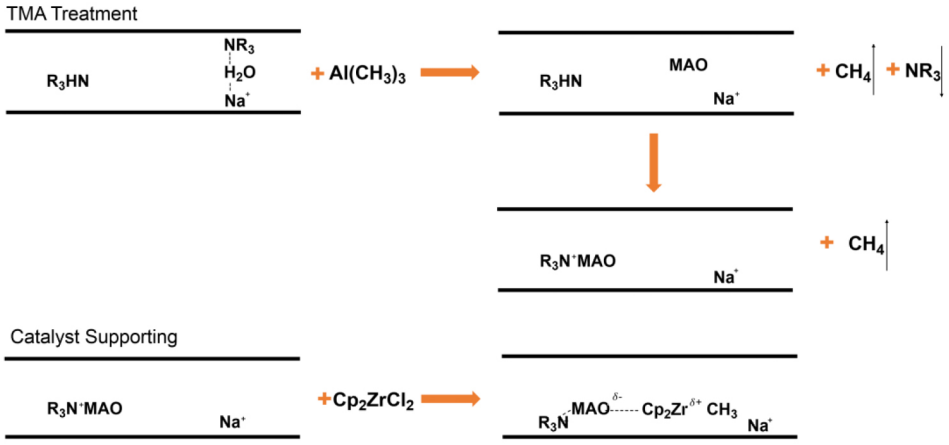

Figure 17. Proposed reactions during catalyst supporting on Cloisite 93A. Adapted from reference 93.

linked to the backbones of a part of the PE chains during ethylene polymerization. In this way, the interfacial interaction between PE and MMT was strengthened, promoting exfoliation of P-MMT lamella in the polymer nanocomposites, and a better dispersion of P-MMTs was achieved in comparison with nonpolymerizable organophilic MMTs. Since the authors found a strong dependence of the dispersion and the concentration of P-MMTs in the reaction systems, a mechanism for the evolution process of the microstructure in PE/P-MMTs nanocomposites was proposed and is shown in Figure 18.

Considering hydroxyl groups as sites for anchoring metallocene catalyst, Wei *et al.*[99] proposed an indirect supporting method: SiO_2 are deposited onto the clay to

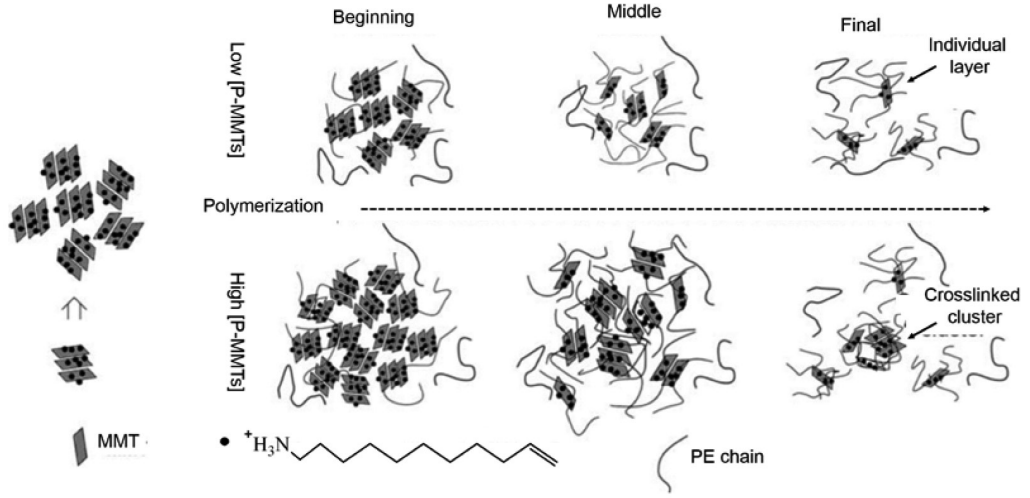

Figure 18. Schematic illustrations of the formation process of PE/P-MMTs nanocomposites during *in situ* ethylene polymerization in the presence of P-MMTs with different concentration. Reprinted with permission from reference 98. Copyright (c) 2014 [John Wiley and Sons, Inc.].

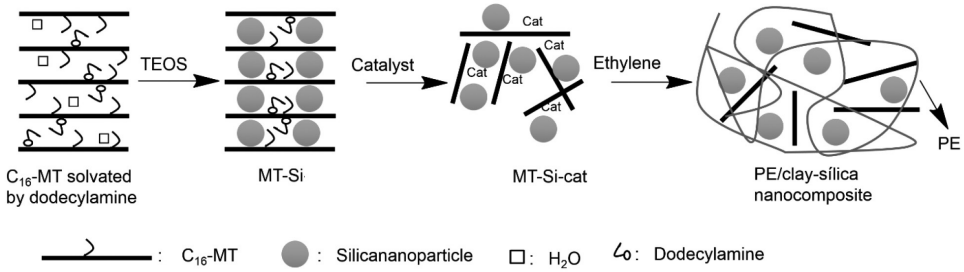

Figure 19. Schematic illustration of mechanism for formation of MT-Si and the PE/clay-silica nanocomposites. Adapted from reference 99.

increase the hydroxyl population on the surface where the loading of active catalyst occurs. For that, MMT is immersed in $MgCl_2$/alcohol solution to promote the diffusion of $MgCl_2$·nROH complexes to the MMT's interlayer space. After removal of the alcohol, $MgCl_2$ is deposited on and between the lamella of MMT. MMT-Si is prepared reacting the treated organically modified MMT (OMMT) with dodecylamine and tetraethylorthosilicate under stirring. After precipitation and drying, the MMT-Si was produced. The MMT-Si-Zr catalyst was prepared reacting the MMT-Si pretreated with MAO with Cp_2ZrCl_2 in toluene. Figure 19 shows the illustration of MMT-Si-Zr and resultant PE nanocomposite.

4. Nanocomposite Preparation

Polymer nanocomposites are two-phase materials in which the polymers are reinforced by nanoscale fillers. This kind of materials have been widely used, both in industry and in academia, in order to improve the mechanical, thermal, barrier, and other properties of the polymer matrix. However, it is widely established that when the fillers are uniformly dispersed in the polymer matrix, the composite properties can be improved to a more dramatic extent. After the preparation of nanocomposites/layered materials, two main types of polymer-filler morphologies can be obtained: intercalated and exfoliated. The intercalated structure occurs from formation of alternate layers of polymer and inorganic layers. An exfoliated structure results when the individual layers are completely separated and dispersed randomly in a polymer matrix.[100] These two types of polymer-layered silicate nanocomposites are shown in Figure 20.

The three most common methods to synthesize NCs are by polymer melt compounding,[102,103] solution blending,[104-106] and intercalation of a suitable monomer and subsequent *in situ* polymerization.[107,108]

4.1. Melt compounding

Melt compounding is the method where a mixture of polymer and filler is annealed above the glass transition

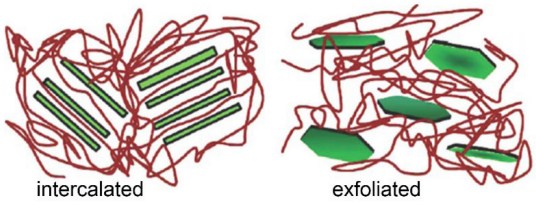

Figure 20. Schematic illustration of two different types of thermodynamically achievable polymer/layered silicate nanocomposites. Reprinted from reference 101. Copyright 2014, with permission from Elsevier.

temperature in either static or flow conditions. This method was first demonstrated by Vaia *et al.*[84] in 1993, that used mica-type layered silicate (MTS) as filler for polystryrene. Using alkylammonium cation as compatibilizer, they obtained the intercalated polymer that is the result of the molecular confinement of the chains within the two-dimensional host galleries.

This method does not require the use of a solvent or monomer, making it simple, economical and environmentally friendly. It demands that a polymer and filler mixture is heated under either batch or continuous shear (i.e., in an extruder) above the softening point of the polymer.[109] During the heating process, the polymer viscosity decreases and allows the diffusion, promoting filler dissemination through the polymer matrix to form either intercalated or exfoliated material, depending on the degree of filler de-aggregation.[110,111] Figure 21 shows an schematic representation of polymer nanocomposite obtained by melt compounding using dimethylbis(hydrogenated-tallow) ammonium montmorillonite [$M_2(HT)_2$]/linear low density PE (LLDPE).[112]

The main drawback of this method is that it often leads to an insufficient filler dispersion, especially at a high filler content, which causes filler aggregation and/or intercalation that, in turn, promotes the deterioration of the mechanical properties, when compared to the corresponding exfoliated nanocomposite. In some cases, *in situ* exfoliation can be achieved during melt mixing, however it is possible only for polymers that can be processed at high temperatures. Usually, the polymer cannot degrade before 230 °C, temperature generally required for exfoliation.[102]

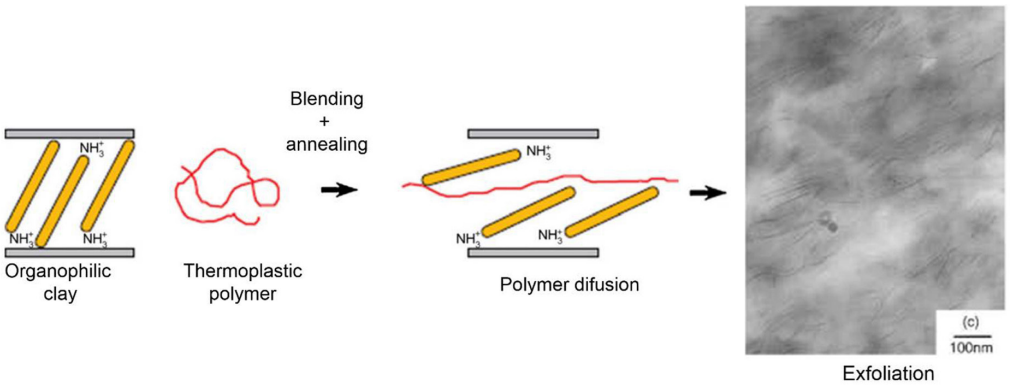

Figure 21. Schematic representation of PLS obtained by direct polymer melt intercalation of $M_2(HT)_2$ with LLDPE. Adapted from references 112 and 113.

Compatibilizers can be used to improve the filler dispersion. Chun *et al.*[11] used a compatibilizer to enhance dispersion of MMT (Cloisite 25A and Cloisite 30B) into the polyurethane (PU) matrix by melt mixing. The authors found that the nanoparticle dispersion was the best at 1 wt.% of MMT and it was improved with compatibilizer content for both tested composites. However, the nanocomposite obtained with Cloisite 25A was significantly affected by the presence of the compatibilizer in contrast to Cloisite 30B, which demonstrated less dependence on the compatibilizer content.

4.2. Solution blending

Polymer nanocomposite preparation by the blending of the filler with the polymer into a solution requires a suitable solvent that can both solubilize the polymer and swell the filler. After the filler is dispersed into the polymer solution, the nanocomposite is obtained upon the removal of the solvent, that can be made by solvent evaporation or polymer precipitation.[114,115] Figure 22 shows an schematic representation of nanocomposite preparation by this method: the case of ethylene vinyl acetate (EVA)/LLDPE/organomodified layered double hydroxide (DS-LDH).[116]

Aranda and Ruiz-Hitzky[118] reported the first preparation of the polyethylene oxide (PEO)/MMT nanocomposites by this method. The authors used different polar solvents, including water, methanol, acetonitrile, and mixtures, to conduct a series of experiments evaluating the influence on intercalation of PEO into Na^+ $^-$MMT. The polarity of the solvents showed to determine the degree of silicate layers that are intercalated by the polymer through this method. The results showed that the high polarity of water helps with the swelling of Na^+ $^-$MMT. Methanol was not suitable as a solvent for PEO, however, water/methanol mixtures promoted intercalation.

The limitation of this method is that it is only applicable to soluble polymers. The use of solvent has the disadvantage of the costs and the environmental impact. Additionally, the polymer solvent must be capable of dispersing the fillers. Kim *et al.*[104] used melt and solvent blending methods to incorporated graphene, derived from graphite oxide (thermally reduced graphene oxide, TRG), via rapid thermal exfoliation and reduction, into LLDPE and its functionalized analogs (with amine, nitrile and isocyanate). They found that graphene was well exfoliated in functionalized LLDPE (represented in Figure 23b), while phase separated morphology was observed in the unmodified LLDPE (represented in Figure 23a). The carbon sheets were more effectively dispersed by solvent blending than by melt compounding. Figure 24 shows the TEM

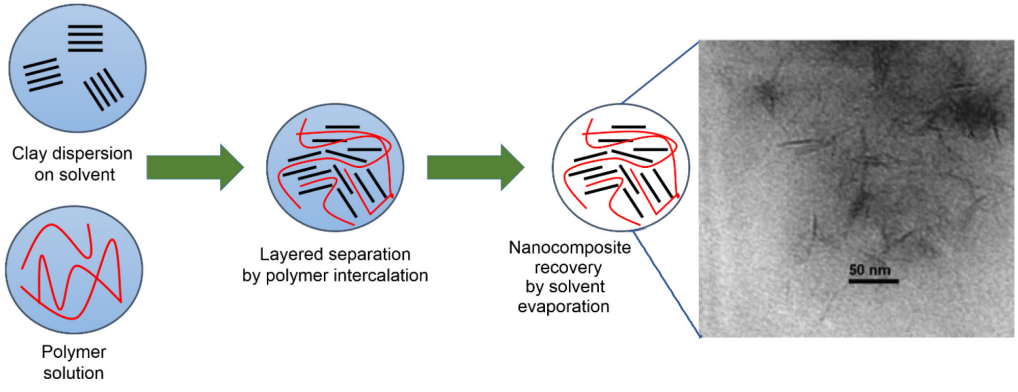

Figure 22. Schematic representation of EVA/LLDPE/DS-LDH obtained by solution blending. Adapted from references 116 and 117.

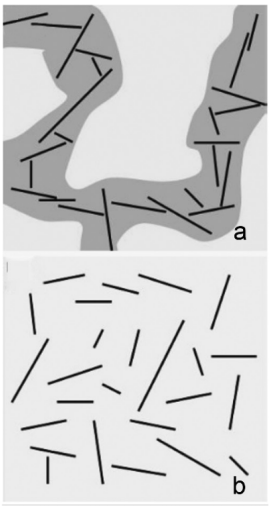

Figure 23. (a) Phase separated and (b) randomly distributed morphology of graphene/polymer nanocomposites. Reprinted from reference 104, Copyright 2014, with permission from Elsevier.

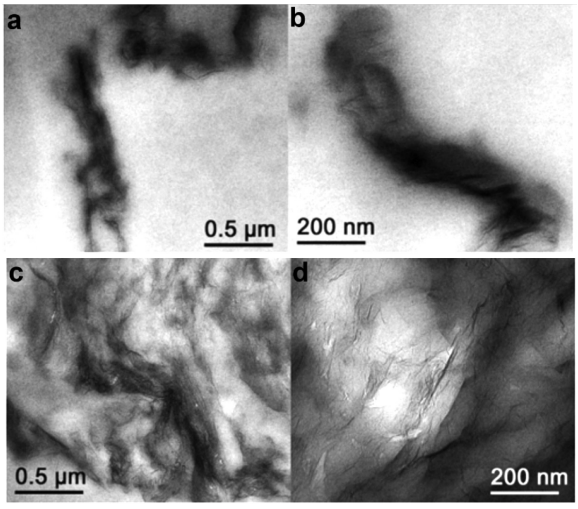

Figure 24. TEM images of 1 wt.% TRG with EG-8200-MA (a, b) prepared by melt compounding and (c, d) prepared by solvent blending. Adapted from reference 104.

micrographs of the LLDPE samples grafted with maleic acid (EG-8200-MA) containing 1 wt.% of TRG prepared by (a, b) melt compound and (c,d) solvent blending.

4.3. *In situ* polymerization

The use of *in situ* polymerization nanocomposite preparation, although not yet established on a large scale, has been shown to give finely-dispersed fillers in polyolefins.[119] In this method, the filler is saturated by the polymer monomer. Subsequent polymerization takes place allowing the formation of polymer chains between the layers of the nanoparticles. Figure 25 shows an schematic representation of nanocomposite production by *in situ* polymerization, using as example PE/OMMT with supported rac-ethylene bis (4,5,6,7-tetra-hydro-1-indenyl) zirconium dichloride.[120]

The pioneering *in situ* polymerization work was made by Toyota researchers toward the development of a N6/MMT nanocomposite.[13,14] The group results showed that, with only very small amounts of layered silicate loadings, the thermal and mechanical properties have been improved remarkably. Lee *et al.*[121] found that polyehtylene terephthalate (PET) obtained by *in situ* polymerization (direct condensation reactions of diol and diacid) in the presence of clay, only produced low Mw polymer nanocomposites. This effect was attributed to a poor control on stoichiometry. Melt intercalation method for the synthesis of PET nanocomposites led only to the production of intercalated nanocomposites. Filler dispersion should be improved. Better results were obtained by using ring-opening polymerization of ethylene terepthalate cyclic oligomers in the presence of organically modified montmorillonites.

The schematic representation of the process that successfully produced PET nanocomposites is shown in Figure 26. The filler interlayers were swollen with cyclic oligomers. Since these cyclic oligomers present low Mw and low viscosity, they could easily intercalate into the filler interlayer spaces, conducting to the increase in the interlayer distance followed by filler delamination.

The general conclusion is that polyolefin nanocomposite preparation by melt compounding and solvent blending

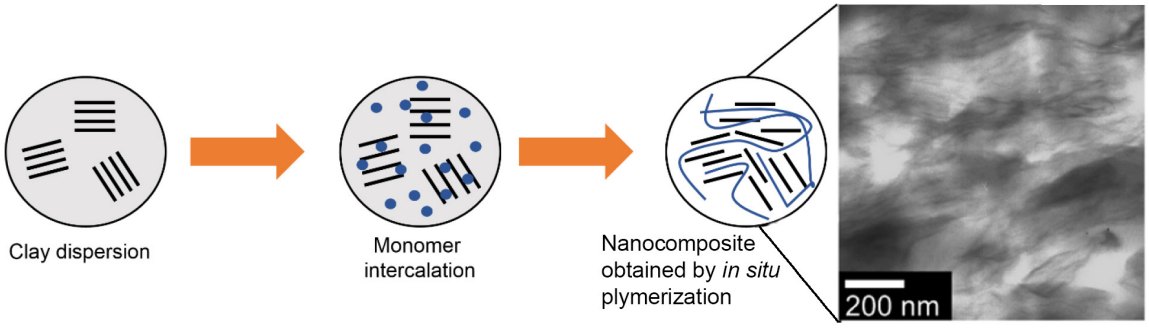

Figure 25. Schematic representation nanocomposite production of PE/OMMT with rac-ethylene bis (4,5,6,7-tetra-hydro-1-indenyl) zirconium dichloride supported obtained by *in situ* polymerization. Adapted from reference 120.

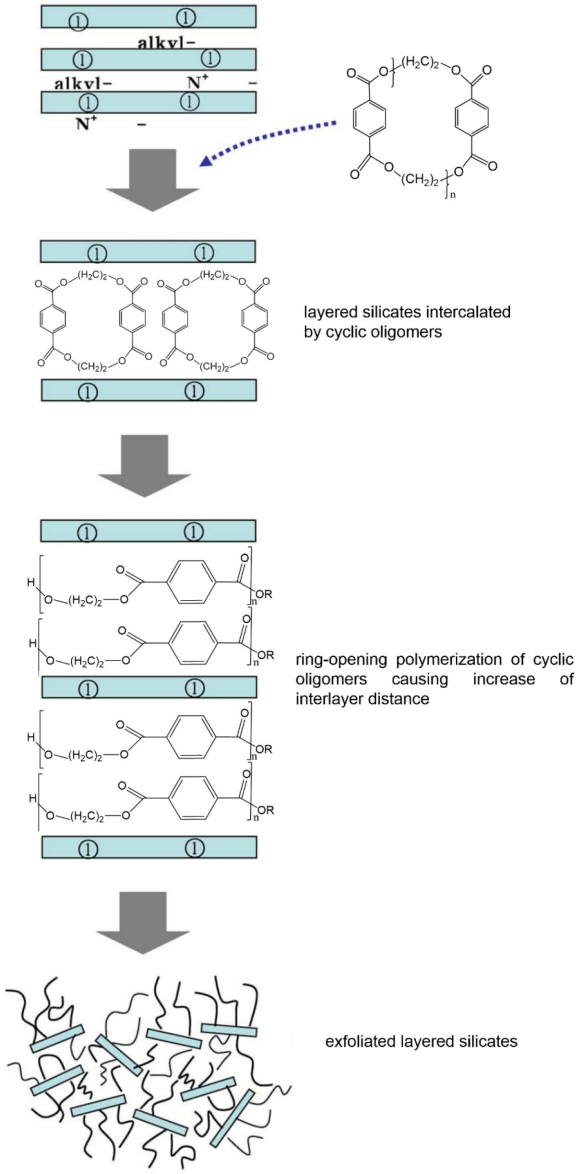

Figure 26. Schematic representation of nanocomposite formation by ring-opening reaction of cyclic oligomers in-between silicate layers. Reprinted from reference 121, Copyright 2014, with permission from Elsevier.

can lead to an insufficient filler dispersion, especially at a high filler content. The main observed problems caused by aggregation and intercalation of the fillers is the deterioration of the mechanical properties of NCs.[3] *In situ* polymerization promotes a better dispersion, whereby the metallocene/methylaluminoxane can be adsorbed or anchored on the surface of the nanofillers such as particles, fibers, layers and tubes and allow the olefin polymerization in the nanoparticle surrounds.

5. Morphological Nanocomposite Properties

The production of NCs promotes superior mechanical, thermal and barrier properties, when comparing with the pristine polymer.[2,122-124] However, these properties are closely related with dispersion of the filler into the polymer matrix.

The structure of nanocomposites are generally determinated by X-ray diffraction (XRD) analysis and TEM. Although XRD analysis offers a convenient method to determine the average interlayer space of layers before and after introduction on nanocomposites, it is impossible to determine the spatial distribution of the layers if it is not organized. Since TEM offers a direct visualization, information about the internal structure, spatial distribution of the phases, and views of the defect structure can be obtained. As can be seen in Figure 27, different morphologies of the inorganic solid support produces different kind of nanocomposite dispersion. By this observation we can conclude that different filler produces different properties on the prepared polymer nanocomposite.

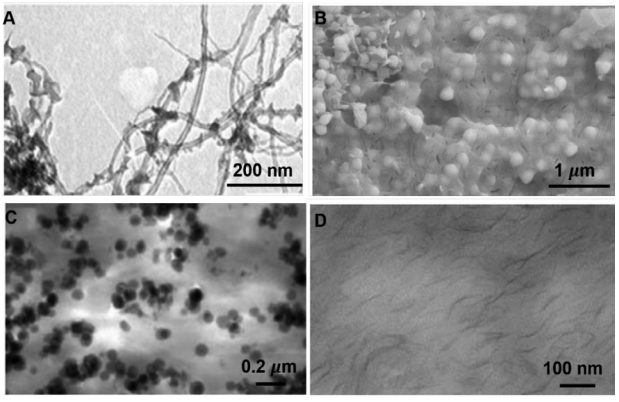

Figure 27. Micrographs of exfoliated nanocomposites composed by (A) PE-coated MWNTs with 12 wt.% by TEM; (B) silica (monospheres) in an isotactic PP matrix prepared with 50 wt.% by SEM; (C) silica (nanospheres) in PE with 7 wt.% by TEM and (D) MMT in a high Mw nylon-6 with 3 wt.% by TEM. Adapted from references 81, 3, 108 and 2, respectively.

Bergman *et al.*[125] successfully produced exfoliated PE-silicate nanocomposite material. The procedure was the intercalation of organically modified fluorohectorite with a well-defined cationic palladium complex. The exposition to the olefin monomer promoted the layers exfoliation (see Figure 28). The confirmation that silicate delamination occurred was made by monitoring the progress of the reaction using powder XRD analysis. The results in Figure 29 show the absence of diffraction peaks after exposure to ethylene for 24 h. This result strongly suggests the formation of an exfoliated polymer nanocomposite.

By the morphological properties, the dispersion related with filler concentration can be determined and then, the respective mechanical and thermal propertied can be analyzed together with filler dispersion. Santos *et al.*[126] evaluated the morphology and properties of PP/organoclay (PP/OMMT) nanocomposites prepared by

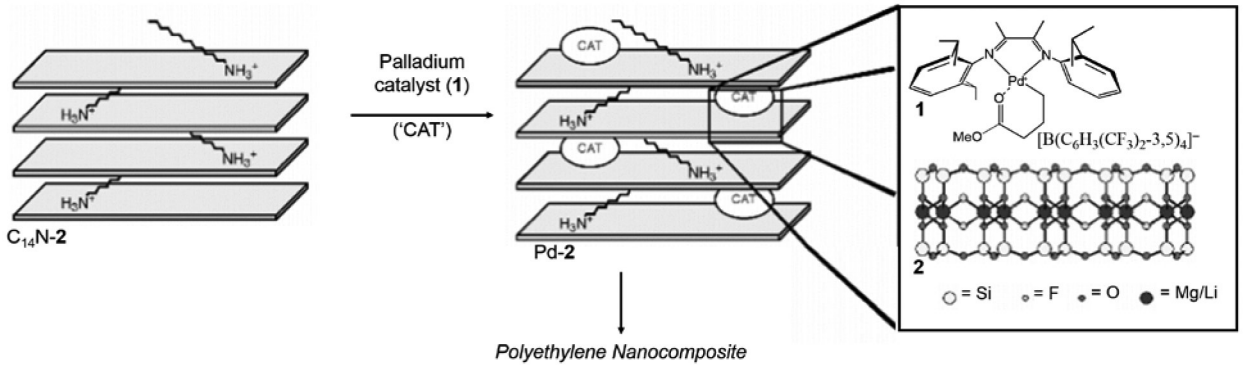

Figure 28. Schematic representation of silicate intercalated by an initiator or catalyst that upon introduction of a monomer an intercalated or exfoliated polymer nanocomposite is formed. Reproduced from reference 125 with permission from The Royal Society of Chemistry.

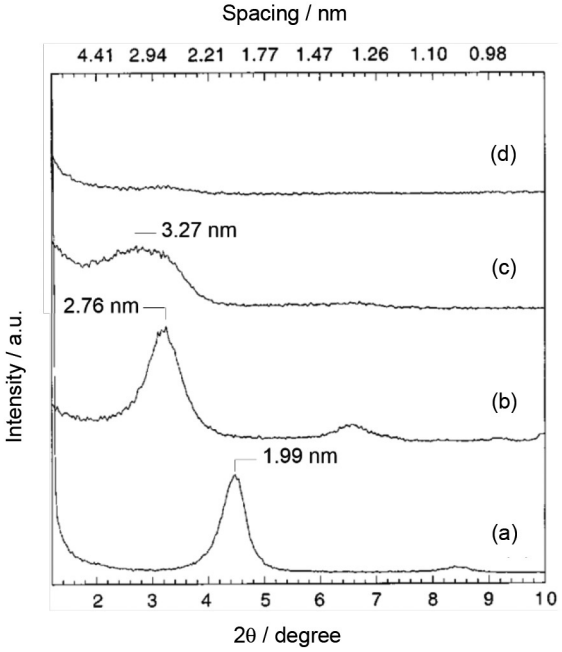

Figure 29. Plot of powder X-ray diffraction intensity *versus* scattering angle: (a) 1-tetradecylammonium modified fluorohectorite (C14N-2); (b) C14N-2 after intercalation by the catalyst (Pd-2); (c) Pd-2 after exposure to ethylene for 135 min; (d) Pd-2 after exposure to ethylene for 24 h. Reproduced from reference 125 with permission from The Royal Society of Chemistry.

melt compounding using maleic anhydride-grafted PP (PP-g-MA) and/or organosilane (OTMS) as compatibilizing agents. They fixed the content of OMMt as 2 wt.%, and tested different concentrations of OTMS, OTMS + PP-g-MA and PP-g-MA. In the absence of the compatibilizer, the PP nanocomposites exhibited agglomerated structures, but when either PP-g-MA or OTMS was added, improved clay dispersion was achieved. Figure 30A shows the TEM image of the sample without the compatibilizer and Figure 30B for the sample with 5% OTMS and 1.5% PP-g-MA. Improvement on layers dispersion by the use of the compatibilizer can be noticed. The authors also discussed the dispersion level promoted by different compatibilizer amounts. Figure 30C shows the image of the sample with 1 wt.% OTMS. It was assigned that the sample with 0.5% OTMS and 1.5% PP-g-MA promoted the best filler dispersion, obtaining exfoliation of the C15A (organophilic montmorillonites Cloisite 15A) platelets in the PP matrix. However, it is difficult to reach such a conclusion analyzing only TEM images, since the dispersions observed by them, with exception of the sample without a compatibilizer (Figure 30A), seems similar. In this case, characterization by another technique is necessary.

Boumbimba *et al.*[127] used PP matrix mixed with several concentrations of organomodified MMT for a comparative study on the extent of the exfoliation by using TEM, XRD, rheological measurements at low frequencies and light scattering measurements. They aimed at providing that the technique of light scattering is capable to measure the degree of exfoliation in polymer nanocomposite systems. By the TEM images, the authors assigned a good dispersion for PPN-0.5 (PP + 0.5 wt.% Nanomax) (Figure 31Aa), and partially exfoliated morphologies are found for higher concentrations, PPN-1.0, PPN-3.0 and PPN-6.0 (Figure 31Ab, 31Ac and 31Ad, respectively). According to the authors, the presence of maleic anhydride increased the compatibility between the PP matrix and the organoclay. However, by the presented images, an assigned of a dispersed system is not possible for any tested samples. The different filler concentrations seem to provide similar effect, non-effectively dispersed layers. Indeed, X-ray diffraction analyses were also made. The results are shown in Figure 31B.

According to the authors, the diffractogram of PPN-0.5 sample showed the disappearance of the broad XRD peak of the nanomax filler. On the XRD patterns, the intercalated structure is evidencied by the increase in basal spacing. Increase from 22.8 Å, for pure nanomax filler, to 28.2 Å and 25.6 Å, for the nanocomposites PPN-3 and PPN-6, respectively, was observed. Considerations about this work, when comparing with the other prepared composites, PPN-0.5 seems to reach the better layer dispersion. However, it was unclear if it really reached the exfoliated statement.

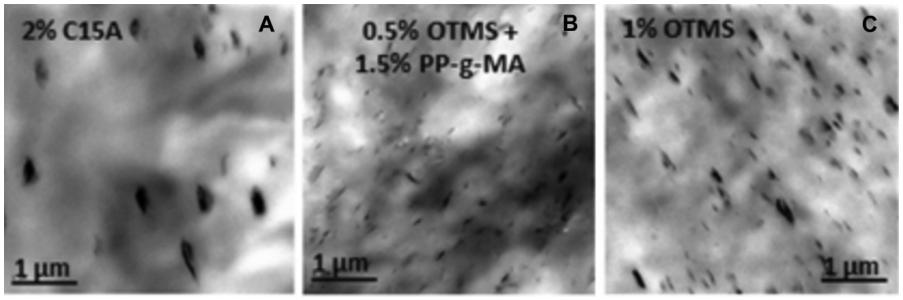

Figure 30. TEM images of the 2 wt.% C15A/PP nanocomposites: without a compatibilizer (A); with 1 wt.% OTMS (B) and with 1.5 wt.% PP-g-MA/0.5 wt.% OTMS (C). Adapted from reference 126.

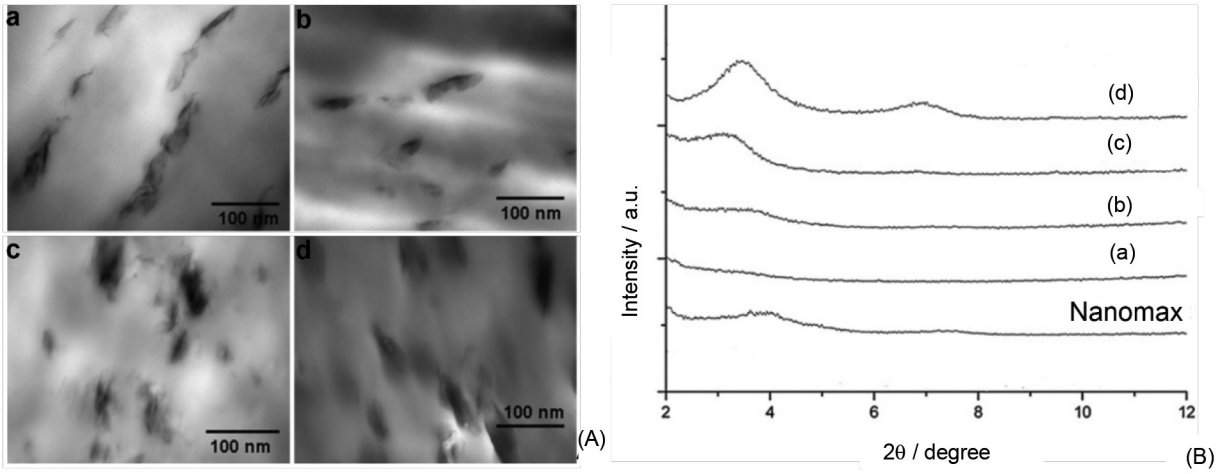

Figure 31. TEM images (A) and XRD patterns (B) of PP nanocomposites with various organoclay contents (a): PPN-0.5; (b) PPN-1; (c) PPN-3; (d) PPN-6. Adapted from reference 127.

Bieligmeyer *et al.*[128] developed a route to obtain fully miscible PE nanocomposites that was established based on polymer-brush-coated nanoparticles. According to the authors, this is a general route to obtain fully miscible nanocomposites with semicrystalline polymers. PE/iron oxide nanoparticles (maghemite) nanocomposites were prepared choosing a ligand exchange procedure and selecting primary amino groups to functionalize the polymer chain-end. As a suggested method, the procedure was based on the polymerization of ethylene in toluene at 80 °C using a neodymocene precatalyst [$Cp^*_2NdCl_2Li(OEt_2)_2$] and butyloctylmagnesium as an activator/chain-transfer agent (CTA) via catalyzed chain growth (CCG). This method was chosen since it allows the control of polymer Mw by the variation of CTA loading and ethylene consumption. Amino-functionalized PE chains were attached to the maghemite nanoparticles via a ligand exchange process. The dispersion degree of nanoparticles within the nanocomposites was characterized by TEM. Figure 32a shows the images of highly filled rhombic PE nanocomposite crystal with 54 wt.% nanoparticles. Magnification shows that the nanoparticles are homogeneous (Figure 32b). PE

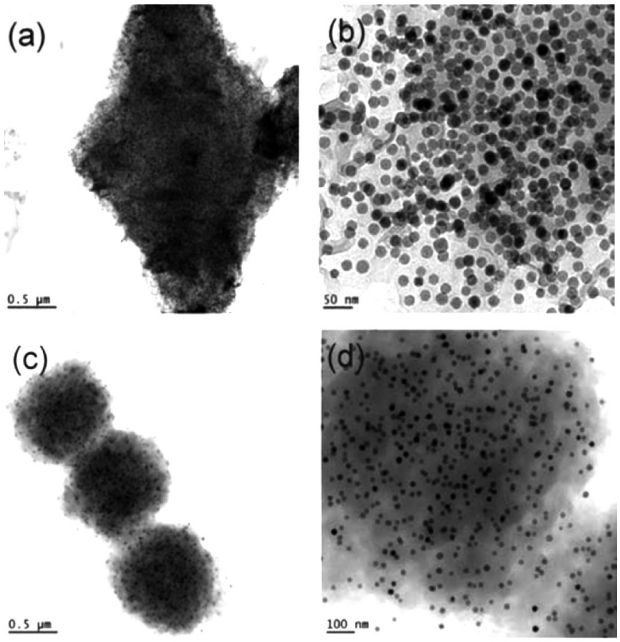

Figure 32. Electron micrographs of a highly filled rhombic PE nanocomposite crystal (54 wt.% nanoparticles) (a) with homogeneous distribution of nanoparticles (b) and of spherical nanocomposite particles for a nanoparticle loading of 7.4 wt.% at low (c) and high (d) magnification. Reprinted with permission from reference 128. Copyright 2014 American Chemical Society.

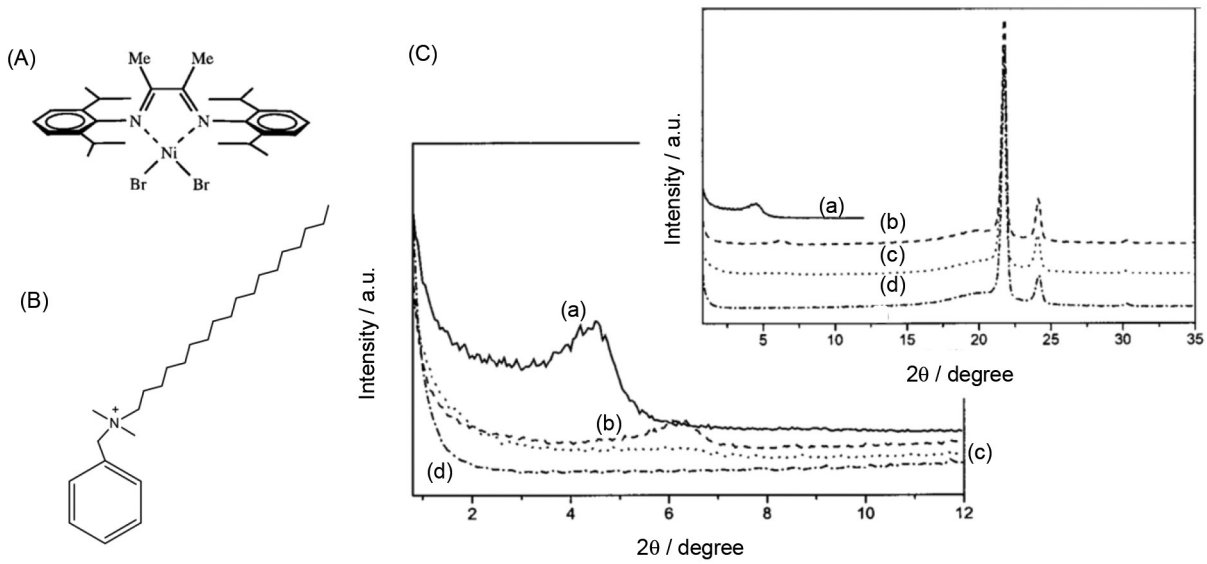

Figure 33. Structures of (A) DMN and (B) dimethylstearylbenzylammonium ions; (C) X-ray diffraction of high density PE nanocomposites: (a) bentonite modified with dimethylstearylbenzylammonium cations; (b) melt-compounded PE/DMSB composite; (c) *in situ* polymerized PE/DMSB nanocomposite; (d) high density PE. Adapted from reference 103.

with 7.4 wt.% of nanoparticles is shown in Figure 32c. The miscibility of the PE-coated nanoparticles with the PE matrix can be seen by the clearly homogeneous distribution of nanoparticles (Figure 32d). The particle sizes were determined by dynamic light scattering and were found to decrease with increasing nanoparticle loading.

The correlation between the method of preparation with the morphological, mechanical and thermal characteristics of the nanocomposites is found in the literature. Heinemann *et al.*[103] polymerizated ethylene using MAO-activated *N*,*N*-bis (2,6-27-diisopropylphenyl)-1,4-diaza-2,3-dimethyl-1,3-butadienenickeldibromide (DMN) (Figure 33A) in toluene. The polymerization process was made in the presence of bentonite modified with dimethylstearylbenzylammonium cations (DMSB) (Figure 33B). X-ray diffraction helped to examine the nanocomposite formation. Figure 33C compares the bulk layered silicate modified with dimethylstearylbenzylammonium ions, curves a, with those of pure polymer, curves d, and polymer nanocomposites prepared by melt compounding, curves b, and *in situ* polymerization, curves c. The study showed that the melt compounding reduced the interlayer spacing characterized by the compression of the silicate layers, attributed by the authors to a non compatibility effect. In contrast, *in situ* polymerization enhanced silicate exfoliation, since the signals from the bentonite modified with dimethylstearylbenzylammonium ions are absent.

TEM images showed the significative improved dispersion of bentonite in the nanocomposites (PE/DMSB),

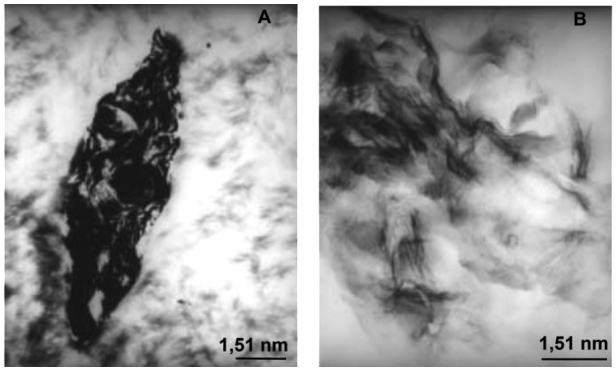

Figure 34. TEM-images of PE/DMSB nanocomposites of high density PE: composite prepared by melt compounding (A) and prepared by *in situ* polymerization (B). Reprinted with permission from reference 103. Copyright (c) 2014 [John Wiley and Sons, Inc.].

prepared by *in situ* polymerization compared with those prepared by melt compounding (Figure 34).

6. Conclusions

Metallocene complexes made important contributions for the PE field. The interest to apply the metallocene complexes supported on inorganic solids comes from industrial interests since the plants operate mainly with heterogeneous Ziegler-Natta catalysis. When the polymerization processes are conducted in the presence of nanoscale inorganic supports, they remain in the final product, leading to the nanocomposites production. Polyolefin nanocomposites represent a huge innovation that brought novel properties and characteristics to the polymers. Polyolefin/clay nanocomposites production has

been receiving special attention due to the improvement on mechanical, thermal and barrier resistance of the polymer.

Properties such as support chemical surface composition, size and shape of the nanoparticles, structure, pore sizes, interlayer distances, hydrophobicity and mechanical, electrical and thermal properties of the fillers have to be taken into account before choosing a desired filler that is supposed, together with the polymer matrix, to reach a determined property. The study of new kinds of inorganic supports, novel anchoring processes to produce new properties and to provide better understanding of nanocomposite for academic purposes is important and should be supported and stimulated.

This review discussed the use of inorganic solid supports for olefin metallocene catalysts and presented the main characteristcs of these materials as well of the metallocene supporting procedure. Several procedures are applied to improve the filler compatibility with the polymer matrix and to reduce the catalyst de-activation. When the ideal treatment procedure is chosen, the nanocomposite production is achieved. Considering that when polymer nanocomposites are compounded with exfoliated nanoparticles, rapid dissipating energy is obtained, then, significative improvements on the properties can be reached. The catalyst, the support, the polymerization conditions and the type of the activator have a profound effect on the catalyst kinetic behavior in the olefin polymerization. The morphology of the nanoparticles also promotes particular changes on final polymer properties.

Above all the considerations about these important topics, it is deeply important, for nanocomposite materials production, that the filler is randomly dispersed on polymer matrix. In order to obtain the desired product characteristics, an important study of the literature about the many influences on filler dispersion must be made. This contribution aimed to discuss, in a general way, the main considerations of the methods cited by published studies and the polymerization application results in the field of polyolefin nanocomposites.

Acknowledgements

The authors gratefully acknowledge the financial support by Fundação de Amparo à Pesquisa no Estado de São Paulo (FAPESP), in the framework of an international pilot project initiated by the IUPAC Polymer Division (FAPESP Grant No. 2010/50385-8) andCoordenação do Pessoal do Nível Superior (CAPES) for the fellowship.

We are indeed lucky when we have colleagues with whom to discuss our work, we are surprised when some of them allow themselves to go deeper into long conversations about our research. However, we are really blessed when we find people like Prof Roberto Fernando de Souza, genuinely available and willing to talk, to present their ideas in a open and intelectually honest fashion. His open and original mind, his generosity led us to the area of supported catalysts for polymerization, where today we find profound intelectual satisfaction.

Aline Cristiane dos Ouros *received her BSc degree in 2009 and her MSc degree in 2011 from the Federal University of Santa Catarina, working with proton exchange membrane fuel cell and electrical conductive polymer nanocomposite production. She is currently completing her PhD in Sciences at the University of Campinas in the Micro- and Mesoporous Molecular Sieves Group, under the supervision of Prof Pastore, working with in situ production of polymer nanocomposites. Her research interests are polymerization, polymer nanocomposites and synthesis of fillers for nanocomposites.*

Michèle Oberson de Souza *is Associated Professor at the Department of Physical-Chemistry of the Institute of Chemistry at the Federal University of Rio Grande do Sul (UFRGS) in Porto Alegre, where she develops her research since 1987. Her main research interests concern the conversion of light olefin oligomerization and polymerization, reactions catalyzed by heterogeneized organometallic systems to improve the production of linear and/or terminal oligomers and special polymers respectively. The grafting of active species onto inorganic nano-structured materials and the development of biphasic processes using ionic liquids are then studded. She is presently co-coordinator of the Laboratory of Reactivity and Catalysis that was, until November 2013, headed by Prof Roberto Fernando de Souza.*

Heloise de Oliveira Pastore *has been based in the Inorganic Chemistry Department, at the Chemistry Institute of the University of Campinas since 1994, where, at the moment, she holds a Full Professor position. Her research interests include the synthesis and modification of micro and mesoporous materials and of layered structures. The organization of molecules and entities at, and by, organo-*

inorganic interfaces is in the core of the group's research. In particular, the transference of properties of lamellar materials to 3D molecular sieves, and vice-versa, through inclusion of heteroatoms in the structures or by topotactic/ hydrothermal conversions has been actively studied by the group. She is presently the scientific coordinator of the Micro- and Mesoporous Molecular Sieves Group.

References

1. Abedi, S.; Abdouss, M.; *Appl. Catal., A* **2014**, *475*, 386.
2. Ray, S. S.; Okamoto, M.; *Prog. Polym. Sci.* **2003**, *28*, 1539.
3. Kaminsky, W.; *Materials* **2014**, *7*, 1995.
4. Vaia, R. A.; Price, G.; Ruth, P. N.; Nguyen, H. T.; Lichtenhan, J.; *Appl. Clay Sci.* **1999**, *15*, 67.
5. Alexandre, M.; Dubois, P.; *Mater. Sci. Eng.* **2000**, *28*, 1.
6. Bharadwaj, R. K.; *Macromolecules* **2001**, *34*, 9189.
7. Giannelis, E. P.; Krishnamoorti, R.; Manias, E.; *Adv. Polym. Sci.* **1999**, *138*, 107.
8. Lebaron, P. C.; Wang, Z.; Pinnavaia, T. J.; *Appl. Clay Sci.* **1999**, *15*, 11.
9. Gilman, J. W.; Jackson, C. L.; Morgan, A. B.; Harris, R.; Manias, E.; Giannelis, E. P.; Wuthenow, M.; Hilton, D.; Phillips, S. H.; Phillips, S. H.; *Chem. Mater.* **2000**, *12*, 1866.
10. Sinclair, K. B.; *Macromol. Symp.* **2001**, *173*, 237.
11. Chun, B. C.; Cho, T. K.; Chong, M. H.; Chung, Y.; Chen, J.; Martin, D.; Cieslinski, R. C.; *J. Appl. Polym. Sci.* **2007**, *106*, 712.
12. Morelos-Gómez, A.; Vega-Díaz, S. M.; González, V. J.; Tristán-López, F.; Cruz-Silva, R.; Fujisawa, K.; Muramatsu, H.; Hayashi, T.; Mi, X.; Shi, Y.; Sakamoto, H.; Khoerunnisa, F.; Kaneko, K.; Sumpter, B. G.; Kim, Y. A.; Meunier, V.; Endo, M.; Muñoz-Sandoval, E.; Terrones, M.; *ACS Nano* **2012**, *6*, 2261.
13. Kojima, Y.; Usuki, A.; Kawasumi, M.; Okada, A.; Fukushima, Y.; Kurauchi, T.; Kamigaito, O.; *J. Mater. Res.* **1993**, *8*, 1185.
14. Usuki, A.; Kojima, Y.; Kawasumi, M.; Okada, A.; Fukushima, Y.; Kurauchi, T.; Kamigaito, O.; *J. Mater. Res.* **1993**, *8*, 1179.
15. Scott, S. L.; Peoples, B. C.; Yung, C.; Rojas, R. S.; Khanna, V.; Sano, H.; Suzuki, T.; Shimizu, F.; *Chem. Commun.* **2008**, 4186.
16. Cui, L.; Woo, S. I.; *Polym. Bull.* **2008**, *61*, 453.
17. Sun, T.; Garcés, J. M.; *Adv. Mater.* **2002**, *14*, 128.
18. Xalter, R.; Pelascini, F.; Mülhaupt, R.; *Macromolecules* **2008**, *41*, 3136.
19. Etcheverry, M.; Ferreira, M. L.; Capiati, N. J.; Pegoretti, A.; Barbosa, S. E.; *Compos. Part A: Appl. Sci. Manuf.* **2008**, *39*, 1915.
20. Breslow, D. S.; *J. Am. Chem. Soc.* **1957**, *79*, 5072.
21. Natta, G.; Pino, P.; Mazzanti, G.; Giannini, U.; *J. Am. Chem. Soc.* **1967**, *79*, 2975.
22. Delferro, M.; Marks, T. J.; *Chem. Rev.* **2011**, *111*, 2450.
23. Kaminsky, W.; Funck, A.; Hähnsen, H.; *Dalton Trans.* **2009**, 3907.
24. Casas, E.; Paredes, B.; Van Grieken, R.; Escola, J. M.; *Catal. Sci. Technol.* **2013**, *3*, 2565.
25. Paredes, B.; Soares, J. B. P.; van Grieken, R.; Carrero, A.; Suarez, I.; *Macromol. Symp.* **2007**, *257*, 103.
26. Alt, H. G.; Köppl, A.; *Chem. Rev.* **2000**, *100*, 1205.
27. Kaminsky, W.; Piel, C.; Scharlach, K.; *Macromol. Symp.* **2005**, *226*, 25.
28. Qiao, J.; Guo, M.; Wang, L.; Liu, D.; Zhang, X.; Yu, L.; Song, W.; Liu, Y.; *Polym. Chem.* **2011**, *2*, 1611.
29. Galli, P.; Vecellio, G.; *Prog. Polym. Sci.* **2001**, *26*, 1287.
30. Soga, K.; Shiono, T.; *Prog. Polym. Sci.* **1997**, *22*, 1503.
31. Sinn, H.; Kaminsky, W.; *Adv. Organomet. Chem.* **1980**, *18*, 99.
32. Wild, F. R. W. P.; Zsolnai, L.; Huttner, G.; Brintzinger, H. H.; *J. Organomet. Chem.* **1982**, *232*, 233.
33. Ewen, J. A.; Jones, R. L.; Razavi, A.; Ferrara, J. D.; *J. Am. Chem. Soc.* **1988**, *110*, 6255.
34. Sinn, H.; *Macromol. Symp.* **1995**, *97*, 27.
35. Kaminsky, W.; *Macromolecules* **2012**, *45*, 3289.
36. Alt, H. G.; *J. Chem. Soc., Dalton Trans.* **1999**, *11*, 1703.
37. Zhang, J.; Jin, G.-X.; *Inorg. Chem. Commun.* **2006**, *9*, 683.
38. Yoon, W. J.; Kim, Y. S.; Kim, I. S.; Choi, K. Y.; *Korean J. Chem. Eng.* **2004**, *21*, 147.
39. De Freitas, A. J. D.; dos Santos, J. H. Z.; Meneghetti, S. M. P.; Meneghetti, M. R.; *J. Appl. Polym. Sci.* **2011**, *119*, 3051.
40. Klapper, M.; Hoffmann, M. S.; Joe, D.; Diesing, T.; Rojas, G.; Naundorf, C.; Fink, G.; Müllen, K.; *Polym. Prepr.* **2011**, *52*, 231.
41. Stürzel, M.; Kurek, A.; Anselm, M.; Halbach, T.; Mülhaupt, R.; *Adv. Polym. Sci.* **2013**, *258*, 279.
42. Hlatky, G. G.; *Chem. Rev.* **2000**, *100*, 1347.
43. Carrado, K. A.; Xu, L.; *Chem. Mater.* **1998**, *10*, 1440.
44. Kuo, S.-W.; Huang, W.-J.; Huang, S.-B.; Kao, H.-C.; Chang, F.-C.; *Polymer* **2003**, *44*, 7709.
45. Dos Santos, J. H. Z.; Krug, C.; da Rosa, M. B.; Stedile, F. C.; Dupont, J.; Forte, M. C.; *J. Mol. Catal. A: Chem.* **1999**, *139*, 199.
46. Carrión, P.; Carrillo-Hermosilla, F.; Alonso-Moreno, C.; Otero, A.; Antiñolo, A.; Sancho, J.; Villaseñor, E.; *J. Mol. Catal. A: Chem.* **2006**, *258*, 236.
47. Galland, G. B.; Seferin, M.; Guimarães, R.; Rohrmann, J. A.; Stedile, F. C.; Santos, J. H. Z.; *J. Mol. Catal. A: Chem.* **2002**, *189*, 233.
48. Kristen, M. O.; *Top. Catal.* **1999**, *7*, 89.
49. Li, K.; Ko, F.; *J. Appl. Polym. Sci.* **2008**, *107*, 1387.
50. Jongsomjit, B.; Panpranot, J.; Praserthdam, P.; *Mater. Lett.* **2007**, *61*, 1376.
51. Li, K.-T.; Kao, Y.-T.; *J. Appl. Polym. Sci.* **2006**, *101*, 2573.
52. Li, K.-T.; Dai, C.-L.; Kuo, C.-W.; *Catal. Commun.* **2007**, *8*, 1209.
53. Li, K.-T.; Kao, Y.-T.; *J. Appl. Polym. Sci.* **2006**, *101*, 2573.
54. Casas, E.; van Grieken, R.; Escola, J. M.; *Appl. Catal., A* **2012**, *437-438*, 44.

55. Van Grieken, R.; Carrero, A.; Suarez, I.; Paredes, B.; *Eur. Polym. J.* **2007**, *43*, 1267.
56. Hicks, J. C.; Mullis, B. A.; Jones, C. W.; *J. Am. Chem. Soc.* **2007**, *129*, 8426.
57. Campos, J. M.; Lourenço, J. P.; Fernandes, A.; Rego, A. M.; Ribeiro, M. R.; *J. Mol. Catal. A: Chem.* **2009**, *310*, 1.
58. Ciardelli, F.; Altomare, A.; Conti, G.; Arribas, G.; Mendez, B.; Ismayel, A.; *Macromol. Symp.* **1994**, *80*, 29.
59. Maschmeyer, T.; Rey, F.; Sankar, G.; Thomas, J. M.; *Nature* **1995**, *378*, 159.
60. Brien, S. O.; Tudor, J.; Maschmeyer, T.; Hare, D. O.; *Chem. Commun.* **1997**, *19*, 1905.
61. Alonso-Moreno, C.; Pérez-Quintanilla, D.; Polo-Cerón, D.; Prashar, S.; Sierra, I.; del Hierro, I.; Fajardo, M.; *J. Mol. Catal. A: Chem.* **2009**, *304*, 107.
62. Rahiala, H.; Beurroies, I.; Eklund, T.; Hakala, K.; Gougeon, R.; Trens, P.; Rosenholm, J. B.; *J. Catal.* **1999**, *188*, 14.
63. Silveira, F.; Alves, M. D. C. M.; Stedile, F. C.; Pergher, S. B. C.; dos Santos, J. H. Z.; *Macromol. React. Eng.* **2009**, *3*, 139.
64. Silveira, F.; Alves, M. D. C. M.; Stedile, F. C.; Pergher, S. B.; Rigacci, A.; dos Santos, J. H. Z.; *J. Mol. Catal. A: Chem.* **2009**, *298*, 40.
65. Marques, M. F. V.; Henriques, C. A.; Monteiro, J. L. F.; Menezes, S. M. C.; Coutinho, F. M. B.; *Macromol. Chem. Phys.* **1997**, *198*, 3709.
66. Marques, M. F. V.; Henriques, C. A.; Monteiro, J. L. F.; Menezes, S. M. C.; Coutinho, F. M. B.; *Polym. Bull.* **1997**, *39*, 567.
67. Michelotti, M.; Arribas, G.; Bronco, S.; Altomare, A.; *J. Mol. Catal. A: Chem.* **2000**, *152*, 167.
68. Costa Vayá, V. I.; Belelli, P. G.; dos Santos, J. H. Z.; Ferreira, M. L.; Damiani, D. E.; *J. Catal.* **2001**, *204*, 1.
69. Covarrubias, C.; Quijada, R.; Rojas, R.; *Appl. Catal., A* **2008**, *347*, 223.
70. Covarrubias, C.; Quijada, R.; Rojas, R.; *Micropor. Mesopor. Mater.* **2009**, *117*, 118.
71. Campos, J. M.; Ribeiro, R. M.; Lourenço, J. P.; Fernandes, A.; *J. Mol. Catal. A: Chem.* **2007**, *277*, 93.
72. Gallo, J. M. R.; Bisio, C.; Marchese, L.; Pastore, H. O.; *Micropor. Mesopor. Mater.* **2011**, *145*, 124.
73. Gallo, J. M. R.; Bisio, C.; Gatti, G.; Marchese, L.; Pastore, H. O.; *Langmuir* **2010**, *26*, 5791.
74. Kageyama, K.; Tamazawa, J.; Aida, T.; *Science* **1999**, *285*, 2113.
75. Tajima, K.; Aida, T.; *Chem. Commun.* **2000**, 2399.
76. Iijima, S.; *Nature* **1991**, *354*, 56.
77. Ajayan, P. M.; *Chem. Rev.* **1999**, *99*, 1787.
78. Baughman, R. H.; Zakhidov, A. A.; de Heer, W. A.; *Science* **2002**, *297*, 787.
79. Park, S.; Yoon, S. W.; Lee, K.-B.; Kim, D. J.; Jung, Y. H.; Do, Y.; Paik, H.; Choi, I. S.; *Macromol. Rapid Commun.* **2006**, *27*, 47.
80. Bredeau, S.; Boggioni, L.; Bertini, F.; Tritto, I.; Monteverde, F.; Alexandre, M.; Dubois, P.; *Macromol. Rapid Commun.* **2007**, *28*, 822.
81. Bonduel, D.; Bredeau, S.; Alexandre, M.; Monteverde, F.; Dubois, P.; *J. Mater. Chem.* **2007**, *17*, 2359.
82. Beyou, E.; Akbar, S.; Chaumont, P.; Cassagnau, P. In *Syntheses and Applications of Carbon Nanotubes and Their Composites*; Suzuri, S., ed.; InTech: Cassagnau, 2013; pp. 77-115.
83. Park, S.; Choi, I. S.; *Adv. Mater.* **2009**, *21*, 902.
84. Tarte, N. H.; Cui, L.; Woo, S.; *Adv. Polym. Sci.* **2013**, *258*, 311.
85. Ray, S. S.; Okamoto, K.; Okamoto, M.; *Macromolecules* **2003**, *36*, 2355.
86. Pinnavaia, T. J.; *Science* **1983**, *220*, 365.
87. Ishida, H.; Campbell, S.; Blackwell, J.; *Chem. Mater.* **2000**, *12*, 1260.
88. Krishnamoorti, R.; Vaia, R. A.; Giannelis, E. P.; *Chem. Mater.* **1996**, *8*, 1728.
89. Ruiz-Hitzky, E.; Aranda, P.; Belver, C. In *Manipulation of Nanoscale Materials: an Introduction to Nanoarchitectonics*; Ariga, K., ed.; RSC: UK, 2012, pp. 87-111.
90. Singla, P.; Mehta, R.; Upadhyay, S. N.; *Green Sustain. Chem.* **2012**, *2*, 21.
91. Koo, C. M.; Kim, M. J.; Choi, M. H.; Kim, S. O.; Chung, I. J.; *J. Appl. Polym. Sci.* **2003**, *88*, 1526.
92. Maneshi, A.; Soares, J. B. P.; Simon, L. C.; *Macromol. Chem. Phys.* **2011**, *212*, 216.
93. Kaminsky, W.; *Macromol. Chem. Phys.* **1996**, *197*, 3907.
94. Ray, S.; Galgali, G.; Lele, A.; Sivaram, S.; *J. Polym. Sci., Part A: Polym. Chem.* **2005**, *43*, 304.
95. Shin, S.-Y. A.; Simon, L. C.; Soares, J. B. P.; Scholz, G.; McKenna, T. F. L.; *Macromol. Symp.* **2009**, *285*, 64.
96. Barrera, E. G.; Stedile, F. C.; de Souza, M. O.; Miranda, M. S. L.; de Souza, R. F.; Bernardo-Gusmão, K.; *Appl. Catal., A* **2013**, *462-463*, 1.
97. Ren, C.; Du, X.; Ma, L.; Wang, Y.; Tang, T.; *J. Appl. Polym. Sci.* **2010**, *117*, 1646.
98. Wei, L.; Tang, T.; Huang, B.; *J. Polym. Sci. Part A: Polym. Chem.* **2004**, *42*, 941.
99. Masenelli-Varlot, K.; Reynaud, E.; Vigier, G.; Varlet, J.; *J. Polym. Sci. Part B: Polym. Phys.* **2002**, *40*, 272.
100. Ray, S. S.; Bousmina, M.; *Prog. Mater. Sci.* **2005**, *50*, 962.
101. Kalaitzidou, K.; Fukushima, H.; Drzal, L. T.; *Compos. Sci. Technol.* **2007**, *67*, 2045.
102. Heinemann, J.; Reichert, P.; Thomann, R.; Mülhaupt, R.; *Macromol. Rapid Commun.* **1999**, *20*, 423.
103. Kim, H.; Kobayashi, S.; AbdurRahim, M. A.; Zhang, M. J.; Khusainova, A.; Hillmyer, M. A.; Abdala, A. A.; Macosko, C. W.; *Polymer* **2011**, *52*, 1837.
104. Chiu, F.-C.; Chu, P.-H.; *J. Polym. Res.* **2006**, *13*, 73.
105. Jiang, L.; Morelius, E.; Zhang, J.; Wolcott, M.; Holbery, J.; *J. Compos. Mater.* **2008**, *42*, 2629.

106. Zhang, X.; Simon, L. C.; *Macromol. Mater. Eng.* **2005**, *290*, 573.
107. Zapata, P. A.; Quijada, R.; Lieberwirth, I.; Benavente, R.; *Macromol. React. Eng.* **2011**, *5*, 294.
108. Vaia, R. A.; Ishii, H.; Giannelis, E. P.; *Chem. Mater.* **1993**, *5*, 1694.
109. Zanetti, M.; Lomakin, S.; Camino, G.; *Macromol. Mater. Eng.* **2000**, *279*, 1.
110. Vaia, R. A.; Giannelis, E. P.; *Macromolecules* **1997**, *30*, 8000.
111. Vaia, R. A.; Giannelis, E. P.; *Polymer* **2001**, *42*, 1281.
112. Hotta, S.; Paul, D. R.; *Polymer* **2004**, *45*, 7639.
113. Beyer, G.; *Plast. Addit. Compd.* **2002**, *4*, 22.
114. Ogata, N.; Kawakage, S.; Ogihara, T.; *J. Appl. Polym. Sci.* **1997**, *66*, 573.
115. Ogata, N.; Jimenez, G.; Kawai, H.; Ogihara, T.; *J. Polym. Sci. Part B: Polym. Phys.* **1997**, *35*, 389.
116. Kuila, T.; Srivastava, S. K.; Bhowmick, A. K.; Saxena, A. K.; *Compos. Sci. Technol.* **2008**, *68*, 3234.
117. Pavlidou, S.; Papaspyrides, C. D.; *Prog. Polym. Sci.* **2008**, *33*, 1119.
118. Aranda, P.; Ruiz-hitzky, E.; *Chem. Mater.* **1992**, *4*, 1395.
119. Meyer, R. S. A.; Luinstra, G. A.; *Adv. Polym. Sci.* **2013**, *258*, 341.
120. Ren, C.; Du, X.; Ma, L.; Wang, Y.; Zheng, J.; Tang, T.; *Polymer* **2010**, *51*, 3416.
121. Lee, S.-S.; Ma, Y. T.; Rhee, H.-W.; Kim, J.; *Polymer* **2005**, *46*, 2201.
122. Ray, S. S.; Okamoto, M.; *Macromol. Rapid Commun.* **2003**, *24*, 815.
123. Bikiaris, D.; *Materials* **2010**, *3*, 2884.
124. Kaminsky, W.; Funck, A.; *Macromol. Symp.* **2007**, *260*, 1.
125. Bergman, J. S.; Chen, H.; Giannelis, E. P.; Thomas, M. G.; Coates, G. W.; *Chem. Commun.* **1999**, *21*, 2179.
126. Santos, K. S.; Liberman, S. A.; Oviedo, M. A. S.; Mauler, R. S.; *J. Mater. Sci.* **2014**, *49*, 70.
127. Matadi Boumbimba, R.; Bouquey, M.; Muller, R.; Jourdainne, L.; Triki, B.; Hébraud, P.; Pfeiffer, P.; *Polym. Test.* **2012**, *31*, 800.
128. Bieligmeyer, M.; Taheri, S. M.; German, I.; Boisson, C.; Probst, C.; Milius, W.; Altstädt, V.; Breu, J.; Schmidt, H.-W.; D'Agosto, F.; Förster, S.; *J. Am. Chem. Soc.* **2012**, *134*, 18157.

Submitted on: August 19, 2014
Published online: October 24, 2014

FAPESP has sponsored the publication of this article.